Nanosilver and the Microbiological Activity of the Particulate Solids versus the Leached Soluble Silver

Journal:	*Nanotoxicology*
Manuscript ID	TNAN-2017-0077.R1
Manuscript Type:	Short Communication
Date Submitted by the Author:	23-Nov-2017
Complete List of Authors:	Faiz, Merisa; The University of New South Wales, School of Chemical Engineering Amal, Rose; The University of New South Wales, School of Chemical Engineering Marquis, Christopher; The University of New South Wales, School of Biotechnology and Biomolecular Sciences Harry, Elizabeth; University of Technology Sydney, ithree Institute Sotiriou, Georgios; Karolinska Institutet, Department of Microbiology, Tumor and Cell Biology Rice, Scott; Nanyang Technological University, The Singapore Centre for Environmental Life Sciences Engineering Gunawan, Cindy; University of Technology Sydney, ithree Institute; The University of New South Wales, School of Chemical Engineering
Keywords:	silver nanoparticles, Ag solids, silver leaching, toxicity, reactive oxygen species
Abstract:	Nanosilver (Ag NPs) is currently one of the most commercialized antimicrobial nanoparticles with as yet, still unresolved cytotoxicity origins. To date, research efforts have mostly described the antimicrobial contribution from the leaching of soluble silver, while the undissolved solid Ag particulates are often considered as being microbiologically inert, serving only as source of the cytotoxic Ag ions. Here, we show the rapid stimulation of lethal cellular oxidative stress in bacteria by the presence of the undissolved Ag particulates. The cytotoxicity characteristics are distinct from those arising from the leached soluble Ag, the latter being locked in

	organic complexes. The work also highlights the unique oxidative stress-independent bacterial toxicity of silver salt. Taken together, the findings advocate that future enquiries on the antimicrobial potency and also importantly, the environmental and clinical impact of Ag NPs use, should pay attention to the potential bacterial toxicological responses to the undissolved Ag particulates, rather than just to the leaching of soluble silver. The findings also put into question the common use of silver salt as model material for evaluating bacterial toxicity of Ag NPs.

Nanosilver and the Microbiological Activity of the Particulate Solids *versus* the Leached Soluble Silver

Merisa B. Faiz[a], Rose Amal[a], Christopher P. Marquis[b], Elizabeth J. Harry[c], Georgios A. Sotiriou[d], Scott A. Rice[e], Cindy Gunawan[a,c*]

[a]*School of Chemical Engineering and* [b]*School of Biotechnology and Biomolecular Sciences, UNSW Australia, Sydney, NSW 2052, Australia;* [c]*ithree institute, University of Technology Sydney, Sydney, NSW 2007, Australia;* [d]*Department of Microbiology, Tumor and Cell Biology, Karolinska Institutet, Stockholm, Sweden;* [e]*The Singapore Centre for Environmental Life Sciences Engineering and School of Biological Sciences, Nanyang Technological University, Singapore.*

*Corresponding author at ithree institute, University of Technology Sydney, Sydney, NSW 2007, Australia. Tel.: +61 295148203. E-mail address: Cindy.Gunawan@uts.edu.au

Nanosilver and the Microbiological Activity of the Particulate Solids *versus* the Leached Soluble Silver

Abstract

Nanosilver (Ag NPs) is currently one of the most commercialized antimicrobial nanoparticles with as yet, still unresolved cytotoxicity origins. To date, research efforts have mostly described the antimicrobial contribution from the leaching of soluble silver, while the undissolved solid Ag particulates are often considered as being microbiologically inert, serving only as source of the cytotoxic Ag ions. Here, we show the rapid stimulation of lethal cellular oxidative stress in bacteria by the presence of the undissolved Ag particulates. The cytotoxicity characteristics are distinct from those arising from the leached soluble Ag, the latter being locked in organic complexes. The work also highlights the unique oxidative stress-independent bacterial toxicity of silver salt. Taken together, the findings advocate that future enquiries on the antimicrobial potency and also importantly, the environmental and clinical impact of Ag NPs use, should pay attention to the potential bacterial toxicological responses to the undissolved Ag particulates, rather than just to the leaching of soluble silver. The findings also put into question the common use of silver salt as model material for evaluating bacterial toxicity of Ag NPs.

Keywords: silver nanoparticles; Ag solids; silver leaching; toxicity; reactive oxygen species

Word count: 6472

Introduction

The rapid development in nanotechnology has seen inorganic nanomaterials such as nanosilver, copper oxide and zinc oxide, subjected to advanced physicochemical manipulation to exhibit powerful antimicrobial activity (Gunawan et al. 2009, 2011, 2013a, Hajipour et al. 2012). Among these materials, nanosilver (silver nanoparticles, Ag NPs) is currently one of the most commercialized due to its potent and broad-spectrum antimicrobial characteristics (Consumer Products Inventory – Project on Emerging Nanotechnologies). Along with applications as core or co-antimicrobial ingredients in wound dressings and internal catheters (Ge et al. 2014), Ag NPs have also been incorporated in an increasing array of consumer products (Deardorff 2014), ranging from personal care products, textiles and household appliances to food and beverages and even children's products (Benn et al. 2010, Quadros et al. 2013). The widespread use is despite the ill-defined antimicrobial mechanisms of Ag NPs, in particular the lack of knowledge regarding the origins of cytotoxicity. The controversy has been at least one of the underlying reasons for regulatory bodies to still classify and regulate Ag NPs as regular bulk silver. Therefore, the nanoparticles are subjected to the same reporting requirements, threshold levels and toxicity tests as bulk silver, despite the mounting evidence indicating differences in their antimicrobial potency and properties (Faunce and Watal 2010). The antimicrobial activity of Ag NPs is influenced by the particles' physicochemical characteristics (*e.g.* size, shape, surface functional groups) as well as interactions with the particles' environment. In real-world settings of Ag NPs antimicrobial applications, the almost inevitable contact of the nanoparticles with aqueous environments, including those in the environment and in the human body, will lead to leaching of soluble silver species through oxidative dissolution of the silver metal (Trop et al. 2006, Benn and Westerhoff 2008, Liu et al. 2012, Sotiriou et al. 2012). Considerable research efforts have described the cytotoxic activity of the leached soluble silver on bacteria, even in their various forms, such as the soluble Ag(I)-chloride anionic complexes (Levard et al. 2013) and organo complexes (Gunawan et al. 2009), as a result of potential interactions of the released

silver with the ubiquitous presence of halides (Cl^-, Br^-, I^-) and biomolecules in the environment and in body fluids (Silver 2003, Liu et al. 2012, Eckhardt et al. 2013). Uncertainty however, still lingers as to the bacterial toxicological responses to the undissolved Ag residue (Gunawan et al. 2009, Sotiriou and Pratsinis 2010, Xiu et al. 2012), that remains after leaching of silver. The solid Ag particulates have been indicated to physically interact with cellular membranes of bacteria (Sondi and Salopek-Sondi 2004, Mirzajani et al. 2011), but otherwise are often regarded as being inert, indirectly contributing to the antimicrobial activity as a source of the cytotoxic Ag ions. This view is inclusive of the hypothesized Trojan-horse type of Ag NPs cytotoxicity, whereby leaching occurs intracellularly following uptake of particles, or, the suggested cell-particle contact to cause additional leaching at the cell-particle interface and in turn, increasing the uptake of Ag ions by bacteria (Lemire et al. 2013, Bondarenko et al. 2013). The elucidation of the source of Ag NPs cytotoxicity will not only clarify the nanoparticles' 'true' antimicrobial potency in real-world applications, but will also contribute to more accurate assessments of their long-term impact on the environment and human health.

Here, we investigated the origins of Ag NPs cytotoxicity through detailed investigations of bacterial toxicological responses to the 'overall' presence of nanosilver (*i.e.* both leached soluble Ag and Ag particulate residue are present in the systems), as compared to those of the corresponding pre-leached filtered Ag leachate samples. Nanosilver in products can be in the forms of nano-sized Ag(I) or metallic Ag^0 coated on or impregnated in support materials (Gunawan et al. 2017). As model material, the current work used nanosilver in the form of nano-sized Ag_2O deposits (d_{TEM} = 2 nm (Gunawan et al. 2009)) homogenously dispersed on the surface of inert TiO_2 support (d_{TEM} = 30 nm (Gunawan et al. 2009)). It is noteworthy to point out that studies have observed discrepancies on the leaching behaviour as well as capability of cellular oxidative stress stimulation of Ag(I) *versus* Ag^0 nanoparticles (Gunawan et al. 2009, Gunawan et al. 2013b). Nonetheless, the generated knowledge of cellular responses to the two

fundamental forms of nanosilver-derived microbiologically active components, that is, the leached soluble silver and the solid Ag particulates in the present study, is relevant to the countless nanosilver design with variation in the particle's properties (*e.g.* size, shape and oxidation states). This facile approach enables unambiguous elucidation of the source of nanoparticulate cytotoxicity without the need to employ simulation materials, such as soluble Ag salt (Gunawan et al. 2009, Sotiriou and Pratsinis 2010, Gunawan et al. 2011, Bondarenko et al. 2013, Ivask et al. 2014), which, as also shown in the current work, exhibits different cytotoxicity characteristics. We report cytotoxic activity of the solid Ag particulates on bacteria, distinct from the leached soluble silver.

Methods

Synthesis of Ag NPs and Preparation of Ag leachate from NPs

The 5 at% Ag/TiO_2 nanoparticles as finely dispersed Ag_2O on inert TiO_2 support were synthesized using the flame spray pyrolysis (FSP) technique as earlier described (Gunawan et al. 2013b, note that at% refers to the percentage of Ag atom relative to the total number of atoms in the particle). TEM images of the particles and XPS spectra that confirm the presence of silver (I) oxide are available (Gunawan et al. 2009). The Ag-leachate was prepared by aseptically pre-dissolving known amounts of Ag NPs (3, 6, 8, 10 mg Ag L^{-1}) in sterile Luria Bertani (LB) broth (5 g L^{-1} yeast extract, 10 g L^{-1} tryptone, 5 g L^{-1} NaCl in deionized water) at 37°C, 280 rpm under dark conditions for 6 h, unsonicated. The undissolved particulates (mean aggregate size = 1.09 ± 0.03 μm by dynamic light scattering (Gunawan et al. 2009)) were removed by centrifugation (5,000 rpm) followed by filtration of the leachate with 0.22 μm polyethersulfone membrane (Millipore Express). Comparable light scattering intensity of the filtered Ag leachate to that of the filtered LB medium confirmed the removal of the solid Ag residue (data not shown). The concentration of soluble silver in the filtered Ag leachate was determined by inductively coupled

plasma mass spectrometry (ICP-MS) (Nexion 300D, PerkinElmer). ICP-MS analysis was also performed on the undissolved Ag residue (3-4 h digestion with 70% (v/v) HNO_3 to dissolve the Ag solid). This Ag solid concentration (no cells) reflected, at least in approximation, the presence of the undissolved Ag fraction in the nanoparticle-bacteria exposure systems (note the comparable leaching of Ag NPs in the presence and absence of bacteria, Figure 1 and S1, Supplementary Data). The ICP-MS analysis of the (digested) solid Ag residue and the corresponding Ag leachate fractions (undigested) found that their concentrations added up (within 10-15%) to the nominal total Ag concentrations of the nanoparticles (Figure S1). Finally, the ICP-MS analysis of digested leachate samples found comparable Ag concentrations before and after digestion, which further validated the removal of the solid Ag residue. Suspended Ag/TiO_2 particulates in the growth medium is expressed as mg L^{-1} to reflect their heterogeneous presence, while the homogeneous nature of soluble Ag is referred to in ppm.

Bacterial Growth Studies with Ag NPs, Ag leachate and $AgNO_3$ salt

The growth experiments on *Bacillus subtilis* strain UNSW 448700 were carried out in triplicate in LB culture medium at 37°C, 280 rpm under dark conditions for 6 h. To prepare the bacterial inoculum, a single agar plate colony was cultured overnight at 30°C, 220 rpm in LB broth. A measured volume of 1-2 mL of the overnight culture (typical OD_{600} of 6-8) was transferred into 50 mL fresh LB broth for a further 0.5-1 h conditioning at 37°C, 280 rpm. For the Ag NPs and $AgNO_3$ exposure, pre-weighed Ag NPs (1.1x of the intended dosage) and 0.5 mL (110x concentrated of the intended dosage) solution of $AgNO_3$ were aseptically added into 50 mL and 49.5 mL LB respectively. The experiments were initiated by the addition of 5 mL bacterial inoculum into the 50 mL broth containing suspended Ag NPs or dissolved silver salt (OD_{600} bacteria initial = 0.04, corresponding to ~2 x 10^7 cfu mL^{-1}). For the Ag leachate exposure, 5 mL of the bacterial inoculum was added into 50 mL LB containing 1.1x concentrated pre-leached Ag

NPs (particle-free). The growth profiles were determined by OD_{600} measurement of the biomass (UV/Vis spectrophotometer, Hitachi U-1100) and the growth inhibiting effects were assessed relative to controls with no added silver. A cell-free silver control (particulates or soluble silver) was employed as a reference to obtain the OD_{600} corresponding to the bacteria. The corresponding leaching profile of Ag NPs during the bacterial exposure was measured by ICP-MS (Nexion 300D, PerkinElmer). For this purpose, a measured volume was sampled from the NPs-exposed culture, centrifuged (5,000 rpm) then filtered with the 0.22 µm membrane to remove the bacteria and Ag solid. The resulting solution was 100x diluted in deionized water and subjected to the ICP-MS analysis.

Detection of Intracellular ROS and Cell Viability

The measurement of cellular ROS generation was performed using the cell permeable oxidative reporter dye H_2DCFDA (2′,7′-dichlorodihydrofluorescein diacetate, Sigma-Aldrich). Following its uptake, cellular esterases cleave the diacetate moieties of H_2DCFDA to form H_2DCF, which readily transforms to the fluorescent DCF when reacts with ROS. The cell viability assay was based on the fluorescent nucleic acid dye propidium iodide (Sigma-Aldrich) staining. PI enters cells with damaged cytoplasmic membrane, while being excluded by healthy cells. Following removal of the culture medium by centrifugation, samples from the Ag NPs, Ag leachate and $AgNO_3$ exposure systems (and the silver-free controls) were washed and re-suspended in sterile saline (8 g L^{-1} NaCl, 0.2 g L^{-1} KCl) at 2.5 x 10^8 CFU mL^{-1}. Independent cellular ROS and cell viability assays were carried out with 10 µM H_2DCFDA and 30 µM PI for 1 h and 15 min respectively, at room temperature under dark conditions. The stained cells were washed with saline and analysed by flow cytometry (FACSCanto™ II, BD Bioscience) at 488 nm excitation with 530 nm and 670 nm emission filter settings for the detection of DCF and PI fluorescence respectively. DCF fluorescence was also measured using a microplate reader (Ensight™ Multimode, Perkin Elmer) at 492 nm and 520 nm excitation and emission filter settings

respectively. The stained cells were also visualized with a BX51WI fluorescence microscope (Olympus) with 460–490 nm excitation filter settings.

Results and discussion

Bacterial growth inhibition: Activity of the solid Ag particulates, the leached soluble Ag and silver salt

To distinguish the cytotoxicity or antimicrobial contribution of the leached soluble Ag and the undissolved Ag particulates, we exposed a model bacteria *B. subtilis* UNSW 448700 to 0 – 10 mg Ag L^{-1} NPs (Ag/TiO_2) and compared the bacterial growth to that of the corresponding leachate-only systems, as a function of soluble silver detected in the exposure systems. The leachate samples were prepared by aseptically pre-dissolving Ag NPs in culture medium followed by removal of the solid Ag residue. Firstly, as shown in Figure 1a, the dose-response growth inhibiting effects of the Ag NPs correlates with the increasing concentration of soluble silver that leached from the NPs. The extent of growth of *B. subtilis* was reduced to ~80% upon exposure to 3 mg Ag L^{-1} NPs (1.3 ppm silver leached into the culture medium at equilibrium) relative to silver-free control cultures after 6 h. The control cultures were characterized by a relatively short lag phase of 1 h, followed by 3 to 4 h active exponential growth phase before entering the stationary phase at 6 h (Figure 1b). Increasing the NPs dosage to 6 mg Ag L^{-1} (2.7 ppm leached Ag) saw 50% bacterial growth, while almost complete growth suppression was observed at MIC_{95} 10 mg Ag L^{-1} NPs exposure (4 ppm leached Ag, see Figure 1b for growth profile, MIC_{95} is minimum inhibitory concentration that cause 5% growth relative to the control). At all of the tested Ag NPs loading, leaching of Ag from NPs was rapid, with detection of ~70% soluble Ag (relative to the leached Ag concentration detected at equilibrium) within 5 min of the Ag NPs-bacterial exposure (see Figure 1c inset for leaching profile of 10 mg Ag L^{-1} NPs). Equilibrium was reached in 1 h with the soluble Ag concentration remained constant afterwards, indicating absence of the Ostwald ripening phenomenon that refers to re-deposition of the

leached Ag on larger particulates (Sotiriou et al. 2012). Increasing the Ag NPs loading saw detection of elevated soluble Ag concentration at equilibrium, with the extent of leaching essentially comparable at 38 – 40% relative to the total added Ag (Figure 1c). This is consistent to earlier studies under comparable conditions (Gunawan et al. 2009, Sotiriou and Pratsinis 2010) with the relatively high degree of leaching was due to, at least in part, the presence of organics in the culture medium as shown later in this study. Note that at all of the tested Ag NPs loadings, similar extent of leaching were observed in the absence of bacteria, therefore excluding the possibility of microbial-induced leaching of Ag (Figure S1).

Despite the correlation between Ag NPs growth inhibiting effects and Ag leaching, a comparison with bacterial growth in the corresponding leachate-only systems yields an interesting observation. Exposure of *B. subtilis* to the pre-leached soluble Ag in fact resulted in much less growth inhibition when compared to those of the corresponding Ag NPs samples (Figure 1a). The presence of ~1.3 ppm Ag leachate for example, was benign to the cultures as they grew to a similar extent as the silver-free control cultures after 6 h. This was in contrast to the ~20% growth reduction of the bacteria when exposed to the corresponding 3 mg Ag L^{-1} NPs with comparable leached soluble Ag content. At higher exposure, the bacterial growth in 4 ppm Ag leachate system was ~85% relative to the control cultures (refer to Figure 1b for growth profile), in contrast to the near complete growth suppression observed in the corresponding 10 mg Ag L^{-1} NPs system. Even doubling the concentration of Ag leachate to 8.3 ppm only slightly reduced the bacterial growth to ~75%. The findings suggest predominant cytotoxicity contribution from the undissolved Ag particulates, rather than that arising from the leached soluble Ag. Further antimicrobial simulation with an equivalent concentration of soluble Ag from $AgNO_3$ salt as shown in Figure 1a, saw more severe growth inhibiting activity of the salt. In the presence of 4 ppm soluble Ag from $AgNO_3$ for example, ~25% *B. subtilis* growth was

observed relative to the control cultures after 6 h (growth profile is shown in Figure 1b), in contrast to the ~85% growth in the leachate system with comparable Ag concentration. Such differences in cytotoxicity may arise from unique cellular physiological responses to the different silver species; the leached soluble Ag and the undissolved Ag particulates from Ag NPs, and the soluble silver from silver salt, as investigated in the following.

Dynamic stimulation of cellular oxidative stress and cell death

We carried out dynamic tracking of intracellular reactive oxygen species (ROS) generation (measured by H_2DCFDA assay) and cell viability (measured by propidium iodide assay, whereby PI enters cells with damaged cytoplasmic membrane, which is indicative of cell death) over the 6 h growth course of *B. subtilis* in the presence of the various forms of silver; the Ag NPs (MIC_{95} 10 mg Ag L^{-1} as reference point, contained 4 ppm leached Ag), its corresponding Ag leachate system (4 ppm Ag) and the equivalent $AgNO_3$ system (4 ppm Ag).

The solid Ag particulates and the leached soluble Ag

At 5 min exposure to 10 mg Ag L^{-1}NPs, a 3-fold higher cellular ROS level was detected in *B. subtilis* relative to the basal ROS levels of the silver-free control cultures, which are by-products of aerobic metabolism in bacteria (Choi and Hu 2008, Gunawan et al. 2011, Eckhardt et al. 2013) (Figure 2a, 2b, 4a). Within 30 min of Ag NPs exposure, the cellular ROS level doubled to ~6-fold of the control. A secondary oxidative stress response, the cellular ROS stimulation has been increasingly realized as one of the major cellular toxicological responses to Ag NPs in bacteria (Choi and Hu 2008, Hwang et al. 2008, Lemire et al. 2013, Gunawan et al. 2013b). The ROS generation is thought to result from destruction of the iron-sulfur [4Fe-4S] clusters of proteins by Ag metal (Xu and Imlay 2012, Lemire et al. 2013) and in turn, releasing the Fenton-active free Fe into the cytoplasm for subsequent reaction with cellular H_2O_2 to produce hydroxyl

radicals ($OH^{\bullet}$) (Imlay et al. 1988). Alternatively, indirect destruction of the iron-sulfur clusters could result from inhibition of respiratory enzymes by Ag NPs in bacteria (Li et al. 2010, 2011). The resulting premature leakage of electrons to oxygen will generate superoxide radicals ($O_2^{\bullet-}$) (Imlay 2003) that in turn again, induces the release of free Fe from iron-sulfur clusters in proteins (Kohanski et al. 2007). Indeed, there have been reports on the cytoplasmic presence of the solid Ag particulates upon bacterial exposure to Ag NPs, as well as the presence of the solids within the bacterial membrane layers (Morones et al. 2005, Grigor'eva et al. 2013, Pal et al. 2007). Here, 75-90% PI-positive non-viable bacteria had been detected within 5 to 30 min exposure to Ag NPs, then close to 100% bactericidal or cell death toxicity at as early as 1 h exposure (Figure 2a, 2b, 4b), which indicates cytoplasmic membrane as one of the target destruction sites of the Ag NPs-stimulated cellular ROS (1-8% non-viable cells were detected in the control cultures over the 6 h growth course) (D'Autreaux et al. 2007, Lemire et al. 2013). As expected, the levels of cellular ROS drastically dropped following the rapid high level stimulation, with the majority if not all of the bacterial population were already killed (Sintubin et al. 2011, Gunawan et al. 2013b). Up to this stage, the data suggest that the generation of high levels of cellular ROS and associated bacteria killing was likely to be responsible for the near complete suppression of *B. subtilis* growth (Figure 1a, 1b).

Interestingly, such cellular ROS stimulation was absent in the bacteria when studied in the corresponding 4 ppm Ag leachate system. Over the 6 h growth course, only basal ROS levels, comparable to those of the silver-free control cultures were detected (Figure 2a, 3a, 4a) and not surprisingly, the little to no changes in the fraction of non-viable cells relative to the control (Figure 2a, 3a, 4b). The stimulation of lethal levels of cellular oxidative stress by the presence of solid Ag particulates therefore suggests their substantial contribution to the cytotoxicity effects observed in the growth studies. Recalling the observed ~15% growth inhibition of the bacteria in

the presence of 4 ppm Ag leachate (Figure 1a, 1b), it would be reasonable to deduce that the exposure only resulted in sub-lethal cytotoxicity, causing a minor fraction of the viable cells uncultivable or slowly proliferating, as further indicated by our growth prediction based on the fraction of viable cells (Figure S2). Indeed, doubling the Ag leachate concentration to 8.3 ppm still saw typical cellular ROS (Figure 3c, 4a inset) and dead cells (Figure 3c, 4b inset) detection as those of the control cultures, despite the slightly higher growth suppression, at ~25% (Figure 1a).

The leached soluble Ag and silver salt

The minimal cellular ROS stimulation was also seen upon exposure of *B. subtilis* to the equivalent 4 ppm soluble Ag from $AgNO_3$. Similar to the 4 ppm Ag leachate system, no elevated level of cellular ROS was observed over the 6 h growth course relative to the control cultures (Figure 2a, 3b, 4a). Unlike the leachate samples however, up to ~40% non-viable cells were detected in the salt system (Figure 3b, 4b), indicating attacks on cytoplasmic membrane (Eckhardt et al. 2013). Considering the comparable Ag content, such discrepancies in cytotoxicity are most likely to result from differences in the chemical speciation of the soluble silver, as herein described. Our Ag NPs leaching study (at the MIC_{95} 10 mg Ag L^{-1} NPs) in the individual culture medium components revealed a characteristic trend of complexation-assisted dissolution of nanoparticles (Gunawan et al. 2011), with higher extent of Ag leaching in the peptide-rich components, in particular tryptone (90% leaching relative to the total added Ag), compared to those in the deionized water (60% leaching) or NaCl (10% leaching) (Figure 4c). A soft Lewis acid, Ag(I) forms silver-peptide complexes upon its release from NPs (Bolea et al. 2014), which is most likely to result from its strong affinity to the NH_x donor groups of histidine (NH^+), arginine ($-NH_2^+$) and lysine ($-NH_3^+$) amino acids and also to the thiol ($-S^-$) donor groups of cysteine and methionine amino acids (Eckhardt et al. 2013). Silver-peptide complexes also form with $AgNO_3$ (Bolea et al. 2014), with a fraction of silver is thought to remain as free ions in

the organic-rich medium (Percival et al. 2005). Thermodynamically feasible, the co-existence of free metal ions and organo metal complexes has been reported for the chemical speciation of soluble copper salts, also a soft Lewis acid metal, in similar culture medium as that used here (Gunawan et al. 2011) (note that the current technology for elemental analysis does not differentiate free Ag ions to those locked in organo complexes (Eckhardt et al. 2013)). When compared to free Ag ions, the hindered transport of the bulkier silver-peptide complexes into bacteria (Solioz and Odermatt 1995) is thought to be at least in part, responsible for the passivated, in this case, sub-lethal cytotoxicity of the Ag leachate. Unlike free Ag ions, research indicates that soluble organo Ag complexes are not recognized by the P-type ATPase transporter present in bacteria (Luoma 2008). As also observed in the current study with the $AgNO_3$ systems, exposure of bacteria to Ag ions has been reported to suppress their proliferation, which was indicated to result from a ROS-independent inhibition of metabolic enzymes (dehydratases) (Xu and Imlay 2012), the lack of cellular ROS stimulation also apparent in this work. Further, complete suppression of *B. subtilis* growth was seen at 8.3 ppm Ag from $AgNO_3$ (Figure 1a), despite there being no change in the fraction of non-viable cells when compared to the 4 ppm Ag exposure (Figure 3d, 4b inset). Our growth prediction based on the fraction of viable cells indicates major presence of non- or slowly proliferating viable cells with the $AgNO_3$ exposure (Figure S2). This loss in replication could also result from the known interactions of Ag ions with DNA in bacteria (most likely with the phosphorus moieties) causing DNA condensation (Feng et al. 2000). The seemingly higher cytotoxic effects of Ag ions as compared to the organo Ag complexes are in agreement with other bacterial studies, whereby extracellular presence of thiol-containing reduced gluthathione (GSH) as silver complexing agent lowered the antimicrobial activity of Ag ions on the Gram-positive *Staphylococcus aureus* and the Gram-negative *Escherichia coli* and *Pseudomonas aeruginosa* (Mulley et al. 2014). Finally, the detection of only basal cellular ROS levels in the $AgNO_3$ exposure systems, even at the double 8.3 ppm Ag (Figure 3d, 4a inset), rules out the oxidative stress stimulation as the main

mechanisms of $AgNO_3$ cytotoxicity. Indeed, studies have found no differences in the antimicrobial activity of Ag ions under aerobic and anaerobic conditions on bacteria (Sintubin et al. 2011).

Conclusions

Here, we report multiple cytotoxicity origins of Ag NPs towards bacteria. Presence of undissolved Ag particulates in a biological environment is not inert. In their presence, rapid generation of lethal cellular ROS levels were detected in bacteria, while the corresponding leached soluble Ag, being locked in organo complexes, only imparts sub-lethal cytotoxicity. The observed differences in bacterial toxicological responses to the solid *versus* soluble Ag corroborate earlier reports on the distinct extent of growth inhibiting activity of the Ag NPs' soluble and solid components (Gunawan et al. 2009, Sotiriou and Pratsinis 2010). With regard to the widespread use of Ag NPs, the resolved unique toxicological responses are expected to result in better recognition of the antimicrobial potency of the nanoparticles in real-world settings and importantly, the long-term impact. Research inquiries have shown elevated and persistent presence of silver in wounds, bladder and even in sewage and estuaries, being associated with the intended or in some cases, accidental release from nanosilver applications; the use of wound dressings, pesticides and washing machines are among the examples (Chen et al. 2004, Trop et al. 2006, Reidy et al. 2013, Donner et al. 2015, Beddow et al. 2017). The current findings imply bacterial toxicological responses to not only the leached soluble Ag, but also the Ag particulates in the microbial habitats. Indeed, studies have observed disruptions in the dynamic and balance of microbial communities from natural aquatic waters upon exposure to nanosilver (Das et al. 2012, Beddow et al. 2017), with the work also detecting presence of soluble Ag and aggregates of Ag from nanosilver in these environmental samples (Beddow et al. 2017). The resolved toxicological responses is key to the elucidation of the recently discovered bacterial potential for adaptation to Ag NPs cytotoxicity (Das et al. 2012, Gunawan et al. 2013b). Finally, the work

highlights the unsuitability of soluble silver salt as model material for Ag NPs cytotoxicity in biological environments, noting a distinct ROS-independent antimicrobial characteristic of soluble Ag when supplied as $AgNO_3$ salt.

Acknowledgments

This work was produced with the financial assistance of the Australian Research Council under the ARC Australian Laureate Fellowship Program and the University of Technology Sydney under the Chancellor's Postdoctoral Research Fellowship Program.

Declaration of interest

The authors declare no conflict of interest.

References

Beddow J, Stolpe B, Cole PA, Lead JR, Sapp M, Lyons BP, et al. 2017. Nanosilver inhibits nitrification and reduces ammoniaoxidising bacterial but not archaeal *amoA* gene abundance in estuarine sediments. Environ Microbiol 19: 500-510.

Benn TM, Westerhoff P. 2008. Nanoparticle silver released into water from commercially available sock fabrics. Environ Sci Technol 42: 4133-4139.

Benn T, Cavanagh B, Hristovski K, Posner JD, Westerhoff P. 2010. The release of nanosilver from consumer products used in the home. J Environ Qual 39: 1875-1882.

Bolea E, Jiménez-Lamana J, Laborda F, Abad-Álvaro I, Bladé C, Arola L, et al. 2014. Detection and characterization of silver nanoparticles and dissolved species of silver in culture medium and cells by AsFIFFF-UV-Vis-ICPMS: application to nanotoxicity tests. Analyst 139: 914-922.

Bondarenko O, Ivask A, Käkinen A, Kurvet I, Kahru A. 2013. Particle-cell contact enhances antibacterial activity of silver nanoparticles. PLoS One 8: e64060.

Chen J, Han CM, Yu CH. 2004. Change in silver metabolism after the application of nanometer silver on burn wound. Chin J Burns 20: 161-163.

Choi O, Hu Z. 2008. Size dependent and reactive oxygen species related nanosilver toxicity to nitrifying bacteria. Environ Sci Technol 42: 4583-4588.

Das P, Williams CJ, Fulthorpe RR, Hoque ME, Metcalfe CD, Xenopoulos MA. 2012. Changes in bacterial community structure after exposure to silver nanoparticles in natural waters. Environ Sci Technol 46: 9120-9128.

D'Autreaux B, Toledano MB. 2007. ROS as signalling molecules: mechanisms that generate specificity in ROS homeostasis. Nat Rev Mol Cell Biol 8: 813-824.

Deardorff J, 2014. Some antibacterials come with worrisome silver lining. Chicago Tribune, 16 Feb. Available from: http://articles.chicagotribune.com/2014-02-16/health/ct-nanosilver-met-20140216_1_consumer-products-other-antibiotic-drugs-germs

Donner E, Scheckel K, Sekine R, Popelka-Filcoff RS, Bennett JW, Brunetti G, et al. 2015. Non-labile silver species in biosolids remain stable throughout 50 years of weathering and ageing. Environ Pollut 205: 78-86.

Eckhardt S, Brunetto PS, Gagnon J, Priebe M, Giese B, Fromm KM. 2013. Nanobio silver: its interactions with peptides and bacteria, and its uses in medicine. Chem Rev 113: 4708-4754.

Faunce T, Watal A. 2010. Nanosilver and global public health: international regulatory issues. Nanomedicine 5: 617-632.

Feng QL, Wu J, Chen GQ, Cui FZ, Kim TN, Kim JO. 2000. A mechanistic study of the antibacterial effect of silver ions on *Escherichia coli* and *Staphylococcus aureus*. J Biomed Mater Res 52: 662-668.

Ge L, Li Q, Wang M, Ouyang J, Li X, Xing MMQ. 2014. Nanosilver particles in medical applications: synthesis, performance, and Toxicity. Int J Nanomed 9: 2399-2407.

Grigor'eva A, Saranina I, Tikunova N, Safonov A, Timoshenko N, Rebrov A, et al. 2013. Fine mechanisms of the interaction of silver nanoparticles with the cells of *Salmonella typhimurium* and *Staphylococcus aureus*. Biometals 26: 479-488.

Gunawan C, Teoh WY, Marquis CP, Lifia J, Amal R. 2009. Reversible antimicrobial photoswitching in nanosilver. Small 5: 341-344.

Gunawan C, Teoh WY, Marquis CP, Amal R. 2011. Cytotoxicity origin of copper(II) oxide nanoparticles: comparative studies with micron-sized particles, leachate, and metal Salts. ACS Nano 5: 7214-7225.

Gunawan C, Teoh WY, Ricardo, Marquis CP, Amal R. 2013a. Zinc oxide nanoparticles induce cell filamentation in *Escherichia coli.* Part Part Syst Charact 30: 375-380.

Gunawan C, Teoh WY, Marquis CP, Amal R. 2013b. Induced adaptation of *Bacillus* sp. to antimicrobial nanosilver. Small 9: 3554-3560.

Gunawan C, Marquis CP, Amal R, Sotiriou GA, Rice SA, Harry EJ. 2017. Widespread and indiscriminate nanosilver use: genuine potential for microbial resistance. ACS Nano 11: 3438-3445.

Hajipour MJ, Fromm KM, Ashkarran AA, Jimenez de Aberasturi D, de Larramendi IR, Rojo T, et al. 2012. Antibacterial properties of nanoparticles. Trends Biotechnol 30: 499-511.

Hwang ET, Lee JH, Chae YJ, Kim YS, Kim BC, Sang BI, et al. 2008. Analysis of the toxic mode of action of silver nanoparticles using stress-specific bioluminescent bacteria. Small 4: 746-750.

Imlay J, Chin S, Linn S. 1988. Toxic DNA damage by hydrogen peroxide through the Fenton reaction *in vitro* and *in vivo*. Science 240: 640-642.

Imlay JA. 2003. Pathways of oxidative damage. Annu Rev Microbiol 57: 395-418.

Ivask A, Elbadawy A, Kaweeteerawat C, Boren D, Fischer H, Ji Z, et al. 2014. Toxicity mechanisms in *Escherichia coli* vary for silver nanoparticles and differ from ionic silver. ACS Nano 8: 374-386.

Kohanski MA, Dwyer DJ, Hayete B, Lawrence CA, Collins JJ. 2007. A common mechanism of cellular death induced by bactericidal antibiotics. Cell 130: 797-810.

Lemire JA, Harrison JJ, Turner RJ. 2013. Antimicrobial activity of metals: mechanisms, molecular targets and applications. Nat Rev Microbiol 11: 371-384.

Levard C, Mitra S, Yang T, Jew AD, Badireddy AR, Lowry GV, et al. 2013. Effect of chloride on the dissolution rate of silver nanoparticles and toxicity to *E. coli*. Environ Sci Technol 47: 5738-5745.

Li WR, Xie XB, Shi QS, Zeng HY, Ou-Yang YS, Chen YB. 2010. Antibacterial activity and mechanism of silver nanoparticles on *Escherichia coli*. Appl Microbiol Biotechnol 85: 1115-1122.

Li WR, Xie XB, Shi QS, Duan SS, Ou-Yang YS, Chen YB. 2011. Antibacterial effect of silver nanoparticles on *Staphylococcus aureus*. Biometals 24: 135-141.

Liu J, Wang Z, Liu FD, Kane AB, Hurt RH. 2012. Chemical transformations of nanosilver in biological environments. ACS Nano 6: 9887-9899.

Luoma SN, 2008. Silver nanotechnologies and the environment: old problems or new challenges? The PEW Charitable Trusts. Available from: https://www.nanotechproject.org/process/assets/files/7036/nano_pen_15_final.pdf [Accessed 11 December 2016]

Mirzajani F, Ghassempour A, Aliahmadi A, Esmaeili MA. 2011. Antibacterial effect of silver nanoparticles on *Staphylococcus aureus*. Res Microbiol 162: 542-549.

Morones JR, Elechiguerra JL, Camacho A, Holt K, Kouri JB, Ramírez JT, et al. 2005. The bactericidal effect of silver nanoparticles. Nanotechnology 16: 2346-2353.

Mulley G, Jenkins ATA, Waterfield NR. 2014. Inactivation of the antibacterial and cytotoxic properties of silver ions by biologically relevant compounds. PLoS One 9: e94409.

Pal S, Tak YK, Song JM. 2007. Does the antibacterial activity of silver nanoparticles depend on the shape of the nanoparticle? A study of the Gram-negative bacterium *Escherichia coli*. Appl Environ Microbiol 73: 1712-1720.

Percival SL, Bowler PG, Russell D. 2005. Bacterial resistance to silver in wound care. J Hosp Infect 60: 1-7.

Quadros ME, Pierson R, Tulve NS, Willis R, Rogers K, Thomas TA, et al. 2013. Release of silver from nanotechnology-based consumer products for children. Environ Sci Technol 47: 8894-8901.

Reidy B, Haase A, Luch A, Dawson KA, Lynch I. 2013. Mechanisms of silver nanoparticle release, transformation and toxicity: a critical review of current knowledge and recommendations for future studies and applications. Materials 6: 2295-2350.

Silver S. 2003. Bacterial silver resistance: molecular biology and uses and misuses of silver compounds. FEMS Microbiol Rev 27: 341-353.

Sintubin L, De Gusseme B, Van der Meeren P, Pycke BFG, Verstraete W, Boon N. 2011. The antibacterial activity of biogenic silver and its mode of action. Appl Microbiol Biotechnol 91: 153-162.

Solioz M, Odermatt A. 1995. Copper and silver transport by CopB-ATPase in membrane vesicles of *Enterococcus hirae*. J Biol Chem 270: 9217-9221.

Sondi I, Salopek-Sondi B. 2004. Silver nanoparticles as antimicrobial agent: a case study on *E. coli* as a model for Gram-negative bacteria. J Colloid Interface Sci 275: 177-182.

Sotiriou GA, Pratsinis SE. 2010.Antibacterial activity of nanosilver ions and particles. Environ Sci Technol 44: 5649-5654.

Sotiriou GA, Meyer A, Knijnenburg JTN, Panke S, Pratsinis SE. 2012. Quantifying the origin of released Ag+ ions from nanosilver. Langmuir 28: 15929−15936.

Trop M, Novak M, Rodl S, Hellbom B, Kroell W, Goessler W. 2006. Silver-coated dressing Acticoat caused raised liver enzymes and argyria-like symptoms in burn patient. J Trauma-Injury Infect Crit Care 60: 648-652.

Xiu ZM, Zhang QB, Puppala HL, Colvin VL, Alvarez PJJ. 2012. Negligible particle-specific antibacterial activity of silver nanoparticles. Nano Lett 12: 4271-4275.

Xu FF, Imlay JA. 2012. Silver(I), mercury(II), cadmium(II), and zinc(II) target exposed enzymic iron-sulfur clusters when they toxify *Escherichia coli*. Appl Environ Microbiol 78: 3614-3621.

Consumer Products Inventory – Project on Emerging Nanotechnologies. Available from: http://www.nanotechproject.org/cpi [accessed 1 March 2017].

Supplementary material is available: Supplementary Figure S1, S2 and S3.

Figure captions

Figure 1. Bacterial growth in the presence of Ag NPs, Ag NPs leachate, silver salt and leaching of Ag NPs. **(a)** Growth of *B. subtilis* (6 h) relative to cell-only control upon exposure to Ag NPs (3, 6, 8, 10 mg Ag L^{-1}), Ag leachate from NPs and $AgNO_3$ as a function of soluble silver detected in the bacterial exposure systems (the growth studies were performed in LB medium). **(b)** Growth profiles of the bacteria in the presence of 10 mg Ag L^{-1} NPs (4 ppm Ag leached into medium at equilibrium), 4 ppm Ag leachate from NPs and 4 ppm Ag from $AgNO_3$. Also shown is the cell-only control growth profile (dashed line). The growth in the presence of Ag was normalised to the extent of growth of the control (in colony forming units, cfu). **(c)** The corresponding equilibrium leaching of Ag NPs in the bacterial exposure systems, shown in the inset is the leaching profile for 10 mg Ag L^{-1} NPs. Each data point in (a), (b), (c) is the average of triplicate experiments with error bars representing the maximum and minimum values detected. The growth studies were performed under dark conditions to render the TiO_2 support

photocatalytically inactive and the benign effect of the TiO_2 support on *B. subtilis* growth had been confirmed (Gunawan et al. 2013b). The growth studies were reproduced on different days with unique bacterial inoculum and particle preparations.

Figure 2. Detection of cellular reactive oxygen species (ROS, H_2DCFDA staining, green cells) and cell death (PI staining, red cells) of *B. subtilis* over its growth course: **(a)** cell-only control and **(b)** in the presence of 10 mg Ag L^{-1} NPs. All stained samples were imaged at comparable cell concentrations (scale bars = 50 µm).

Figure 3. Detection of cellular reactive oxygen species (ROS, H_2DCFDA staining, green cells) and cell death (PI staining, red cells) of *B. subtilis* over its growth course, in the presence of: **(a)** 4 ppm Ag leachate from NPs (equivalent leachate to 10 mg Ag L^{-1} NPs exposure), **(b)** 4 ppm Ag from $AgNO_3$, **(c)** 8.3 ppm Ag leachate from NPs and **(d)** 8.3 ppm Ag from $AgNO_3$. All stained samples were imaged at comparable cell concentrations (scale bars = 50 µm).

Figure 4. **(a)** Dynamic stimulation of cellular ROS in *B. subtilis* measured by H_2DCFDA assay over its growth course (5, 30 min and 1, 3, 4.5, 6 h) upon exposure to 10 mg Ag L^{-1} NPs (4 ppm Ag leached into medium at equilibrium), 4 ppm Ag leachate from NPs and 4 ppm Ag from $AgNO_3$. The detected cellular ROS was normalised to the basal ROS levels of the cell-only control growth. Shown in the inset is cellular ROS detected in the presence of 8.3 ppm Ag leachate from NPs and 8.3 ppm Ag from $AgNO_3$. **(b)** The corresponding dynamic cell death detection probed by PI staining of *B. subtilis* throughout its growth course. Also shown is the fraction of dead cells detected for the cell-only control. Statistical analysis of the data was performed with one-way ANOVA followed by Dunnett's posthoc analysis in Prism (GraphPad) (Figure S3). The experiments in (a) and (b) were reproduced on different days with unique bacterial inoculum and particle preparations. **(c)** Leaching profile of 10 mg Ag L^{-1} NPs in cell-

free individual components of the Luria Bertani (LB) culture medium (5 g L^{-1} NaCl, 5 g L^{-1} yeast extract, 10 g L^{-1} tryptone dissolved in deionized water). Each data point in (a), (b), (c) is the average of triplicate batches with the error bars representing the maximum and minimum.

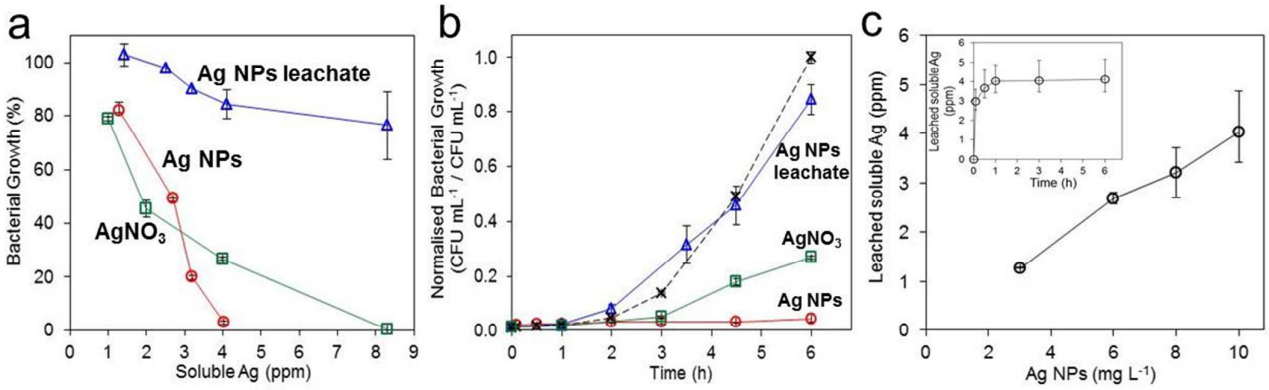

Figure 1

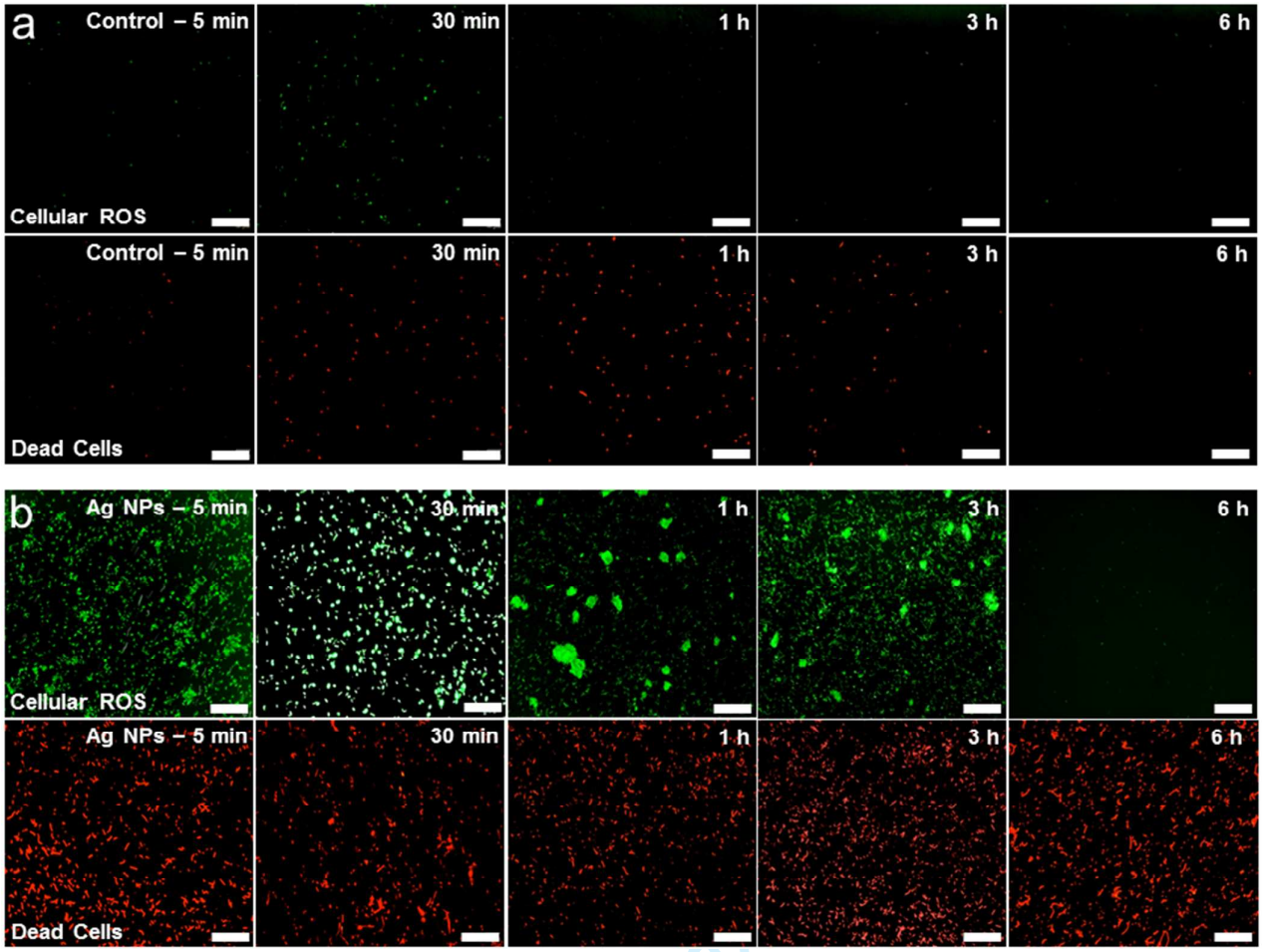

Figure 2

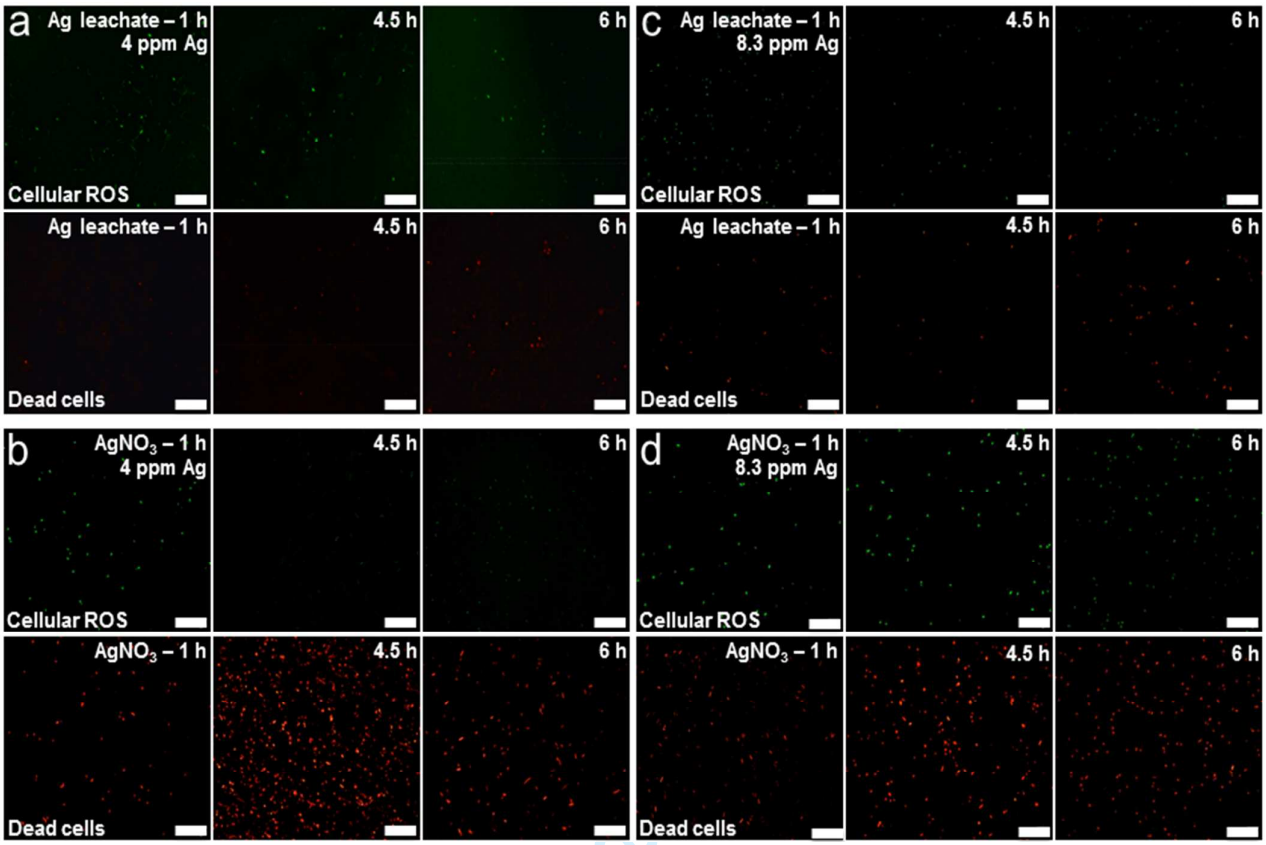

Figure 3

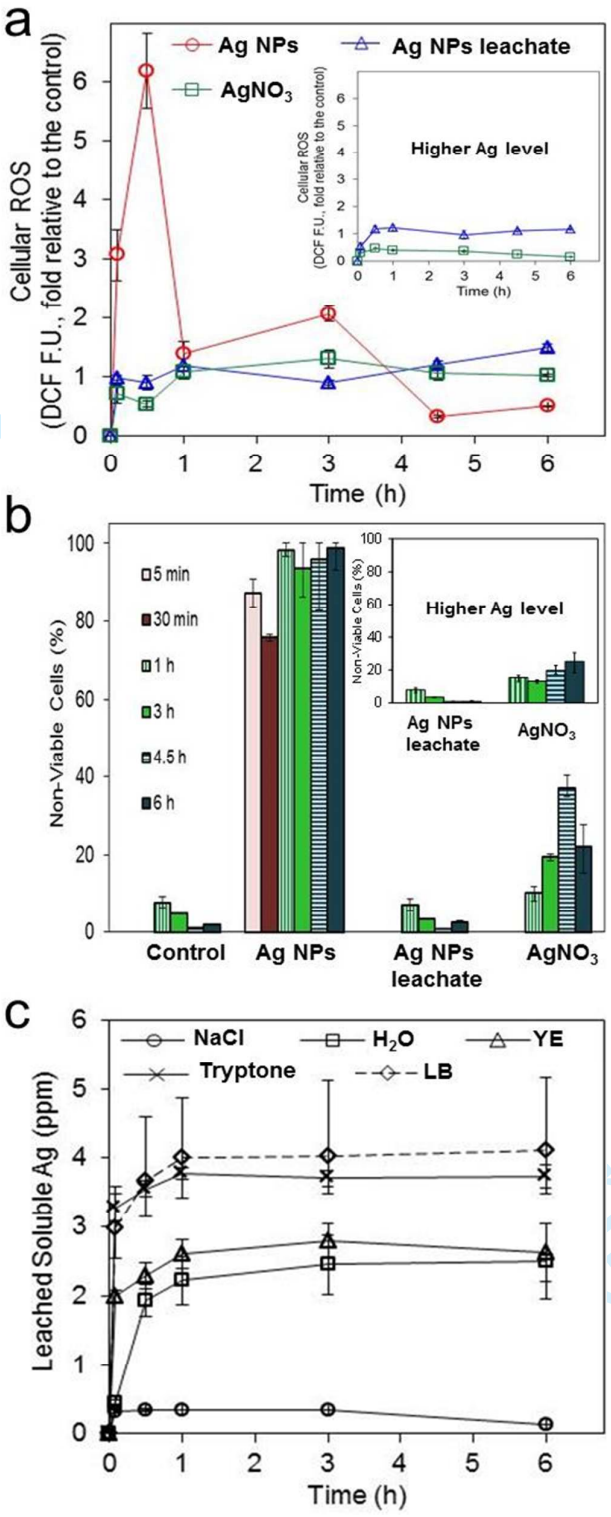
a
Ag NPs
Ag NPs leachate
AgNO3
Higher Ag level
Cellular ROS (DCF F.U., fold relative to the control)
Time (h)
b
5 min
30 min
1 h
3 h
4.5 h
6 h
Non-Viable Cells (%)
Higher Ag level
Control
Ag NPs
Ag NPs leachate
AgNO3
c
NaCl
H2O
YE
Tryptone
LB
Leached Soluble Ag (ppm)
Time (h)

Figure 4

Nanosilver and the Microbiological Activity of the Particulate Solids *versus* the Leached Soluble Silver

Merisa B. Faiz[1], Rose Amal[1], Christopher P. Marquis[2], Elizabeth J. Harry[3], Georgios A. Sotiriou[4], Scott A. Rice[5], Cindy Gunawan[1,3*]

Supplementary Data

Quantification of the soluble and solid Ag fractions

ICP-MS analysis was performed to determine the concentration of the leached soluble Ag and the undissolved Ag particulate residue of the Ag NPs-culture medium systems (no cells).

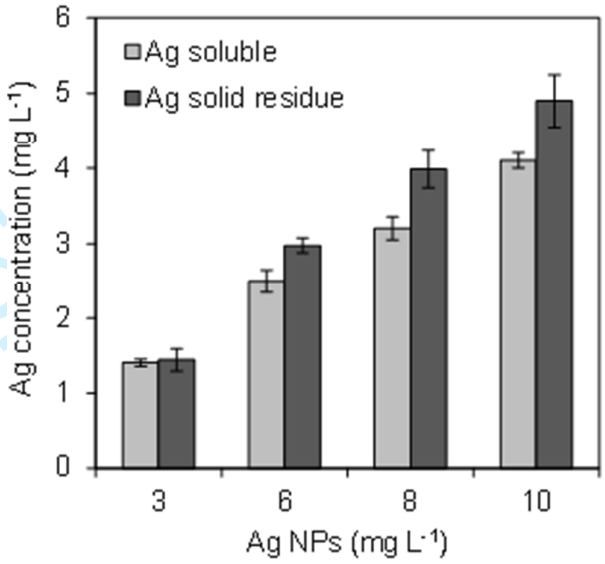

Figure S1. Concentration of the soluble and solid Ag fractions of the Ag NPs-culture medium systems (no bacteria), samples were taken at 6 h following NPs addition.

First order kinetic prediction of growth upon exposure to Ag leachate from NPs and $AgNO_3$

The presence of non- or slowly proliferating viable cells as a result of exposure of *B. subtilis* to 4 and 8.3 ppm Ag leachate as well as to the equivalent 4 and 8.3 ppm soluble Ag from $AgNO_3$ salt is validated by overestimation of the predicted biomass growth based on first order kinetic, *i.e.* $[A_n] / [A_{n-1}] = e^{kt}$, where $[A_{n-1}]$ is the concentration of PI-negative (viable) cells at previous time interval. The rate coefficient (k) is estimated from bacteria-only control growth.

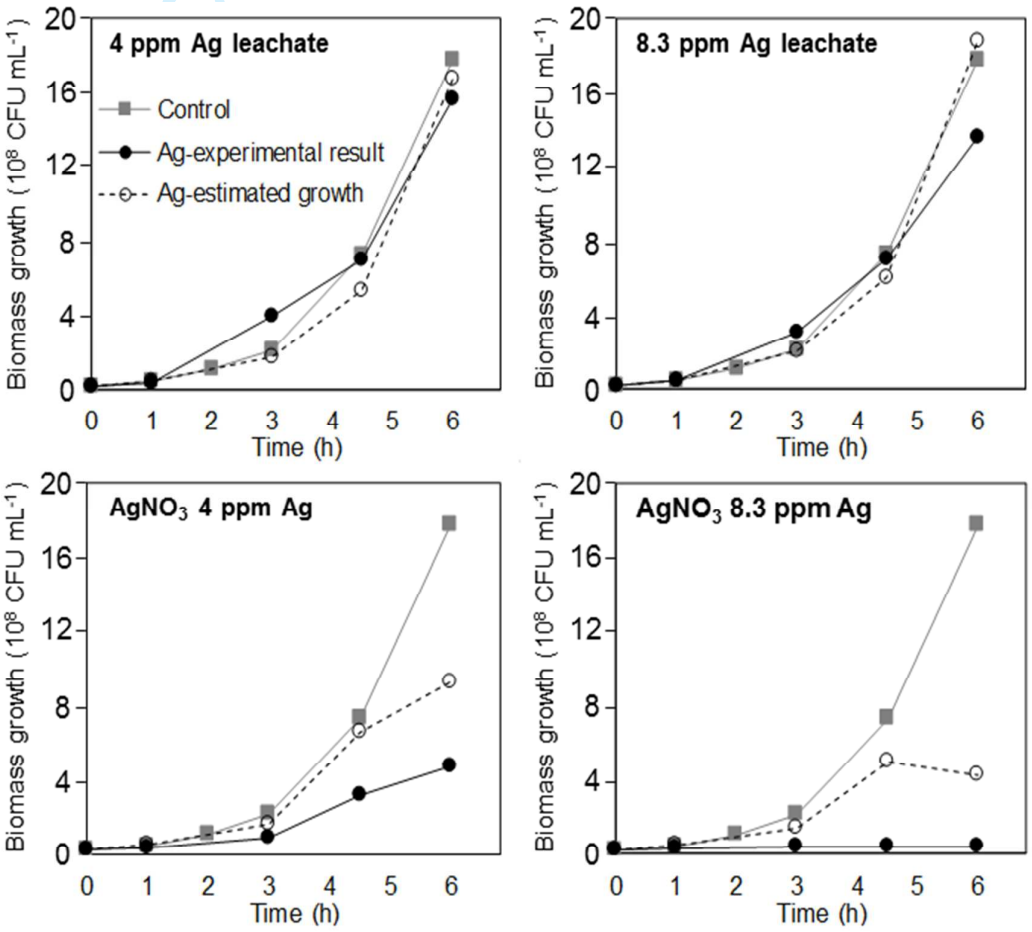

Figure S2. First order kinetic growth prediction of *B. subtilis* upon exposure to 4 & 8.3 ppm Ag NPs leachate and to 4 & 8.3 ppm Ag from $AgNO_3$ as compared to the actual growth.

Statistical analysis of silver-induced cellular reactive oxygen species generation and cell death detection

The statistical significance of cytotoxicity of Ag NPs, Ag NPs leachate and $AgNO_3$ relative to the bacteria-only control was analyzed by using a one-way ANOVA followed by Dunnett's posthoc analysis in Prism (GraphPad).

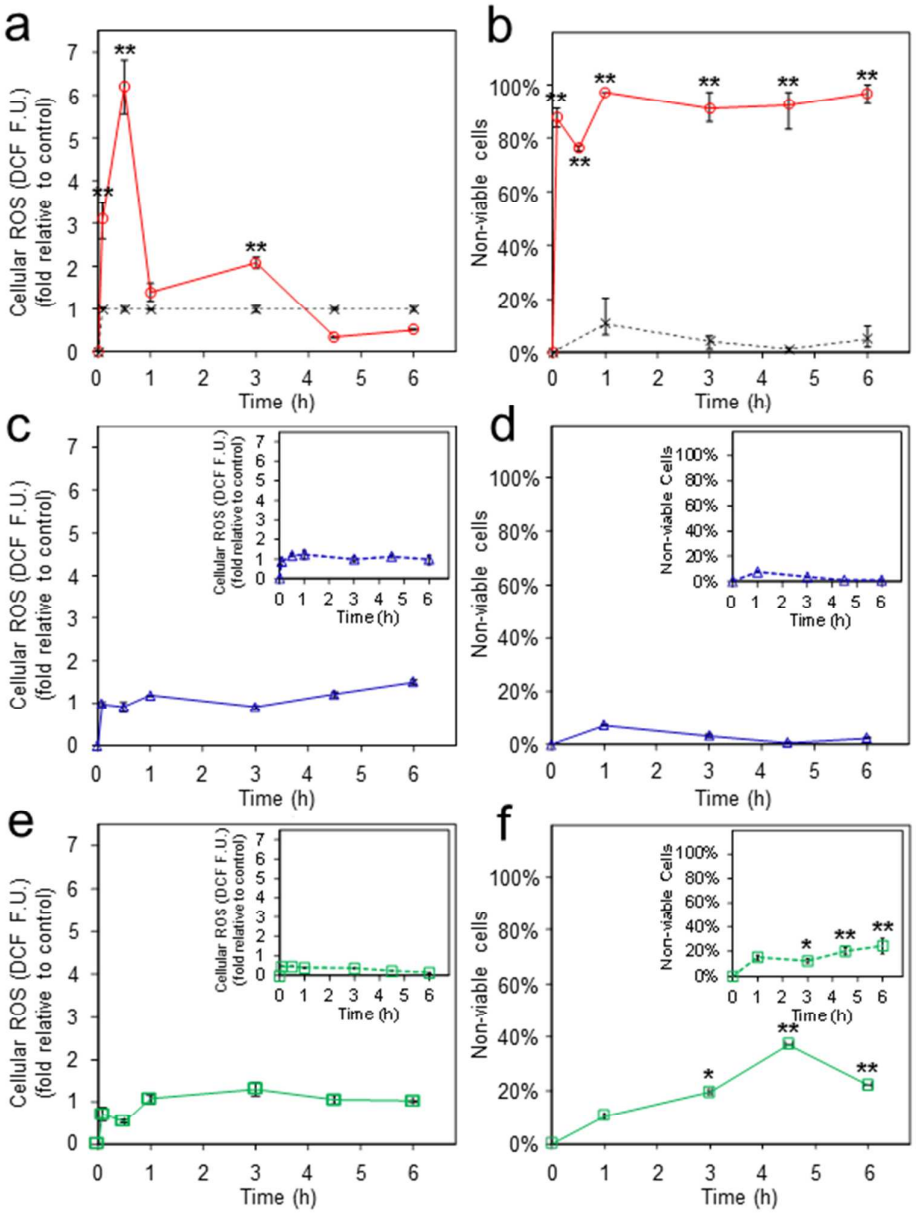

Figure S3. Statistical analysis of dynamic cellular ROS and cell death detection over the course of *B. subtilis* growth upon exposure to (a, b) 10 mg Ag L^{-1} NPs (4 ppm Ag leached into medium

at equilibrium) (c, d) 4 ppm Ag leachate from NPs (inset is 8.3 ppm Ag leachate from NPs) (e, f) 4 ppm Ag from $AgNO_3$ (inset is 8.3 ppm Ag from $AgNO_3$). The asterisks (*, **) correspond to p values of ≤ 0.01, 0.001 respectively, and indicate statistical significance relative to the bacteria-only control (dashed lines).

Nanosilver and the Microbiological Activity of the Particulate Solids *versus* the Leached Soluble Silver

Merisa B. Faiz[a], Rose Amal[a], Christopher P. Marquis[b], Elizabeth J. Harry[c], Georgios A. Sotiriou[d], Scott A. Rice[e], Cindy Gunawan[a,c*]

[a]*School of Chemical Engineering and* [b]*School of Biotechnology and Biomolecular Sciences, UNSW Australia, Sydney, NSW 2052, Australia;* [c]*ithree institute, University of Technology Sydney, Sydney, NSW 2007, Australia;* [d]*Department of Microbiology, Tumor and Cell Biology, Karolinska Institutet, Stockholm, Sweden;* [e]*The Singapore Centre for Environmental Life Sciences Engineering and School of Biological Sciences, Nanyang Technological University, Singapore.*

*Corresponding author at ithree institute, University of Technology Sydney, Sydney, NSW 2007, Australia. Tel.: +61 295148203. E-mail address: Cindy.Gunawan@uts.edu.au

Nanosilver and the Microbiological Activity of the Particulate Solids *versus* the Leached Soluble Silver

Abstract

Nanosilver (Ag NPs) is currently one of the most commercialized antimicrobial nanoparticles with as yet, still unresolved cytotoxicity origins. To date, research efforts have mostly described the antimicrobial contribution from the leaching of soluble silver, while the undissolved solid Ag particulates are often considered as being microbiologically inert, serving only as source of the cytotoxic Ag ions. Here, we show the rapid stimulation of lethal cellular oxidative stress in bacteria by the presence of the undissolved Ag particulates. The cytotoxicity characteristics are distinct from those arising from the leached soluble Ag, the latter being locked in organic complexes. The work also highlights the unique oxidative stress-independent bacterial toxicity of silver salt. Taken together, the findings advocate that future enquiries on the antimicrobial potency and also importantly, the environmental and clinical impact of Ag NPs use, should pay attention to the potential bacterial toxicological responses to the undissolved Ag particulates, rather than just to the leaching of soluble silver. The findings also put into question the common use of silver salt as model material for evaluating bacterial toxicity of Ag NPs.

Keywords: silver nanoparticles; Ag solids; silver leaching; toxicity; reactive oxygen species

Word count: 6472

Introduction

The rapid development in nanotechnology has seen inorganic nanomaterials such as nanosilver, copper oxide and zinc oxide, subjected to advanced physicochemical manipulation to exhibit powerful antimicrobial activity (Gunawan et al. 2009, 2011, 2013a, Hajipour et al. 2012). Among these materials, nanosilver (silver nanoparticles, Ag NPs) is currently one of the most commercialized due to its potent and broad-spectrum antimicrobial characteristics (Consumer Products Inventory – Project on Emerging Nanotechnologies). Along with applications as core or co-antimicrobial ingredients in wound dressings and internal catheters (Ge et al. 2014), Ag NPs have also been incorporated in an increasing array of consumer products (Deardorff 2014), ranging from personal care products, textiles and household appliances to food and beverages and even children's products (Benn et al. 2010, Quadros et al. 2013). The widespread use is despite the ill-defined antimicrobial mechanisms of Ag NPs, in particular the lack of knowledge regarding the origins of cytotoxicity. The controversy has been at least one of the underlying reasons for regulatory bodies to still classify and regulate Ag NPs as regular bulk silver. Therefore, the nanoparticles are subjected to the same reporting requirements, threshold levels and toxicity tests as bulk silver, despite the mounting evidence indicating differences in their antimicrobial potency and properties (Faunce and Watal 2010). The antimicrobial activity of Ag NPs is influenced by the particles' physicochemical characteristics (*e.g.* size, shape, surface functional groups) as well as interactions with the particles' environment. In real-world settings of Ag NPs antimicrobial applications, the almost inevitable contact of the nanoparticles with aqueous environments, including those in the environment and in the human body, will lead to leaching of soluble silver species through oxidative dissolution of the silver metal (Trop et al. 2006, Benn and Westerhoff 2008, Liu et al. 2012, Sotiriou et al. 2012). Considerable research efforts have described the cytotoxic activity of the leached soluble silver on bacteria, even in their various forms, such as the soluble Ag(I)-chloride anionic complexes (Levard et al. 2013) and organo complexes (Gunawan et al. 2009), as a result of potential interactions of the released

silver with the ubiquitous presence of halides (Cl^-, Br^-, I^-) and biomolecules in the environment and in body fluids (Silver 2003, Liu et al. 2012, Eckhardt et al. 2013). Uncertainty however, still lingers as to the bacterial toxicological responses to the undissolved Ag residue (Gunawan et al. 2009, Sotiriou and Pratsinis 2010, Xiu et al. 2012), that remains after leaching of silver. The solid Ag particulates have been indicated to physically interact with cellular membranes of bacteria (Sondi and Salopek-Sondi 2004, Mirzajani et al. 2011), but otherwise are often regarded as being inert, indirectly contributing to the antimicrobial activity as a source of the cytotoxic Ag ions. This view is inclusive of the hypothesized Trojan-horse type of Ag NPs cytotoxicity, whereby leaching occurs intracellularly following uptake of particles, or, the suggested cell-particle contact to cause additional leaching at the cell-particle interface and in turn, increasing the uptake of Ag ions by bacteria (Lemire et al. 2013, Bondarenko et al. 2013). The elucidation of the source of Ag NPs cytotoxicity will not only clarify the nanoparticles' 'true' antimicrobial potency in real-world applications, but will also contribute to more accurate assessments of their long-term impact on the environment and human health.

Here, we investigated the origins of Ag NPs cytotoxicity through detailed investigations of bacterial toxicological responses to the 'overall' presence of nanosilver (*i.e.* both leached soluble Ag and Ag particulate residue are present in the systems), as compared to those of the corresponding pre-leached filtered Ag leachate samples. Nanosilver in products can be in the forms of nano-sized Ag(I) or metallic Ag^0 coated on or impregnated in support materials (Gunawan et al. 2017). As model material, the current work used nanosilver in the form of nano-sized Ag_2O deposits (d_{TEM} = 2 nm (Gunawan et al. 2009)) homogenously dispersed on the surface of inert TiO_2 support (d_{TEM} = 30 nm (Gunawan et al. 2009)). It is noteworthy to point out that studies have observed discrepancies on the leaching behaviour as well as capability of cellular oxidative stress stimulation of Ag(I) *versus* Ag^0 nanoparticles (Gunawan et al. 2009, Gunawan et al. 2013b). Nonetheless, the generated knowledge of cellular responses to the two

fundamental forms of nanosilver-derived microbiologically active components, that is, the leached soluble silver and the solid Ag particulates in the present study, is relevant to the countless nanosilver design with variation in the particle's properties (*e.g.* size, shape and oxidation states). This facile approach enables unambiguous elucidation of the source of nanoparticulate cytotoxicity without the need to employ simulation materials, such as soluble Ag salt (Gunawan et al. 2009, Sotiriou and Pratsinis 2010, Gunawan et al. 2011, Bondarenko et al. 2013, Ivask et al. 2014), which, as also shown in the current work, exhibits different cytotoxicity characteristics. We report cytotoxic activity of the solid Ag particulates on bacteria, distinct from the leached soluble silver.

Methods

Synthesis of Ag NPs and Preparation of Ag leachate from NPs

The 5 at% Ag/TiO_2 nanoparticles as finely dispersed Ag_2O on inert TiO_2 support were synthesized using the flame spray pyrolysis (FSP) technique as earlier described (Gunawan et al. 2013b, note that at% refers to the percentage of Ag atom relative to the total number of atoms in the particle). TEM images of the particles and XPS spectra that confirm the presence of silver (I) oxide are available (Gunawan et al. 2009). The Ag-leachate was prepared by aseptically pre-dissolving known amounts of Ag NPs (3, 6, 8, 10 mg Ag L^{-1}) in sterile Luria Bertani (LB) broth (5 g L^{-1} yeast extract, 10 g L^{-1} tryptone, 5 g L^{-1} NaCl in deionized water) at 37°C, 280 rpm under dark conditions for 6 h, unsonicated. The undissolved particulates (mean aggregate size = 1.09 ± 0.03 µm by dynamic light scattering (Gunawan et al. 2009)) were removed by centrifugation (5,000 rpm) followed by filtration of the leachate with 0.22 µm polyethersulfone membrane (Millipore Express). Comparable light scattering intensity of the filtered Ag leachate to that of the filtered LB medium confirmed the removal of the solid Ag residue (data not shown). The concentration of soluble silver in the filtered Ag leachate was determined by inductively coupled

plasma mass spectrometry (ICP-MS) (Nexion 300D, PerkinElmer). ICP-MS analysis was also performed on the undissolved Ag residue (3-4 h digestion with 70% (v/v) HNO_3 to dissolve the Ag solid). This Ag solid concentration (no cells) reflected, at least in approximation, the presence of the undissolved Ag fraction in the nanoparticle-bacteria exposure systems (note the comparable leaching of Ag NPs in the presence and absence of bacteria, Figure 1 and S1, Supplementary Data). The ICP-MS analysis of the (digested) solid Ag residue and the corresponding Ag leachate fractions (undigested) found that their concentrations added up (within 10-15%) to the nominal total Ag concentrations of the nanoparticles (Figure S1). Finally, the ICP-MS analysis of digested leachate samples found comparable Ag concentrations before and after digestion, which further validated the removal of the solid Ag residue. Suspended Ag/TiO_2 particulates in the growth medium is expressed as mg L^{-1} to reflect their heterogeneous presence, while the homogeneous nature of soluble Ag is referred to in ppm.

Bacterial Growth Studies with Ag NPs, Ag leachate and $AgNO_3$ salt

The growth experiments on *Bacillus subtilis* strain UNSW 448700 were carried out in triplicate in LB culture medium at 37°C, 280 rpm under dark conditions for 6 h. To prepare the bacterial inoculum, a single agar plate colony was cultured overnight at 30°C, 220 rpm in LB broth. A measured volume of 1-2 mL of the overnight culture (typical OD_{600} of 6-8) was transferred into 50 mL fresh LB broth for a further 0.5-1 h conditioning at 37°C, 280 rpm. For the Ag NPs and $AgNO_3$ exposure, pre-weighed Ag NPs (1.1x of the intended dosage) and 0.5 mL (110x concentrated of the intended dosage) solution of $AgNO_3$ were aseptically added into 50 mL and 49.5 mL LB respectively. The experiments were initiated by the addition of 5 mL bacterial inoculum into the 50 mL broth containing suspended Ag NPs or dissolved silver salt (OD_{600} bacteria initial = 0.04, corresponding to ~2 x 10^7 cfu mL^{-1}). For the Ag leachate exposure, 5 mL of the bacterial inoculum was added into 50 mL LB containing 1.1x concentrated pre-leached Ag

NPs (particle-free). The growth profiles were determined by OD_{600} measurement of the biomass (UV/Vis spectrophotometer, Hitachi U-1100) and the growth inhibiting effects were assessed relative to controls with no added silver. A cell-free silver control (particulates or soluble silver) was employed as a reference to obtain the OD_{600} corresponding to the bacteria. The corresponding leaching profile of Ag NPs during the bacterial exposure was measured by ICP-MS (Nexion 300D, PerkinElmer). For this purpose, a measured volume was sampled from the NPs-exposed culture, centrifuged (5,000 rpm) then filtered with the 0.22 µm membrane to remove the bacteria and Ag solid. The resulting solution was 100x diluted in deionized water and subjected to the ICP-MS analysis.

Detection of Intracellular ROS and Cell Viability

The measurement of cellular ROS generation was performed using the cell permeable oxidative reporter dye H_2DCFDA (2′,7′-dichlorodihydrofluorescein diacetate, Sigma-Aldrich). Following its uptake, cellular esterases cleave the diacetate moieties of H_2DCFDA to form H_2DCF, which readily transforms to the fluorescent DCF when reacts with ROS. The cell viability assay was based on the fluorescent nucleic acid dye propidium iodide (Sigma-Aldrich) staining. PI enters cells with damaged cytoplasmic membrane, while being excluded by healthy cells. Following removal of the culture medium by centrifugation, samples from the Ag NPs, Ag leachate and $AgNO_3$ exposure systems (and the silver-free controls) were washed and re-suspended in sterile saline (8 g L^{-1} NaCl, 0.2 g L^{-1} KCl) at 2.5 x 10^8 CFU mL^{-1}. Independent cellular ROS and cell viability assays were carried out with 10 µM H_2DCFDA and 30 µM PI for 1 h and 15 min respectively, at room temperature under dark conditions. The stained cells were washed with saline and analysed by flow cytometry (FACSCanto™ II, BD Bioscience) at 488 nm excitation with 530 nm and 670 nm emission filter settings for the detection of DCF and PI fluorescence respectively. DCF fluorescence was also measured using a microplate reader (Ensight™ Multimode, Perkin Elmer) at 492 nm and 520 nm excitation and emission filter settings

respectively. The stained cells were also visualized with a BX51WI fluorescence microscope (Olympus) with 460–490 nm excitation filter settings.

Results and discussion

Bacterial growth inhibition: Activity of the solid Ag particulates, the leached soluble Ag and silver salt

To distinguish the cytotoxicity or antimicrobial contribution of the leached soluble Ag and the undissolved Ag particulates, we exposed a model bacteria *B. subtilis* UNSW 448700 to 0 – 10 mg Ag L^{-1} NPs (Ag/TiO_2) and compared the bacterial growth to that of the corresponding leachate-only systems, as a function of soluble silver detected in the exposure systems. The leachate samples were prepared by aseptically pre-dissolving Ag NPs in culture medium followed by removal of the solid Ag residue. Firstly, as shown in Figure 1a, the dose-response growth inhibiting effects of the Ag NPs correlates with the increasing concentration of soluble silver that leached from the NPs. The extent of growth of *B. subtilis* was reduced to ~80% upon exposure to 3 mg Ag L^{-1} NPs (1.3 ppm silver leached into the culture medium at equilibrium) relative to silver-free control cultures after 6 h. The control cultures were characterized by a relatively short lag phase of 1 h, followed by 3 to 4 h active exponential growth phase before entering the stationary phase at 6 h (Figure 1b). Increasing the NPs dosage to 6 mg Ag L^{-1} (2.7 ppm leached Ag) saw 50% bacterial growth, while almost complete growth suppression was observed at MIC_{95} 10 mg Ag L^{-1} NPs exposure (4 ppm leached Ag, see Figure 1b for growth profile, MIC_{95} is minimum inhibitory concentration that cause 5% growth relative to the control). At all of the tested Ag NPs loading, leaching of Ag from NPs was rapid, with detection of ~70% soluble Ag (relative to the leached Ag concentration detected at equilibrium) within 5 min of the Ag NPs-bacterial exposure (see Figure 1c inset for leaching profile of 10 mg Ag L^{-1} NPs). Equilibrium was reached in 1 h with the soluble Ag concentration remained constant afterwards, indicating absence of the Ostwald ripening phenomenon that refers to re-deposition of the

leached Ag on larger particulates (Sotiriou et al. 2012). Increasing the Ag NPs loading saw detection of elevated soluble Ag concentration at equilibrium, with the extent of leaching essentially comparable at 38 – 40% relative to the total added Ag (Figure 1c). This is consistent to earlier studies under comparable conditions (Gunawan et al. 2009, Sotiriou and Pratsinis 2010) with the relatively high degree of leaching was due to, at least in part, the presence of organics in the culture medium as shown later in this study. Note that at all of the tested Ag NPs loadings, similar extent of leaching were observed in the absence of bacteria, therefore excluding the possibility of microbial-induced leaching of Ag (Figure S1).

Despite the correlation between Ag NPs growth inhibiting effects and Ag leaching, a comparison with bacterial growth in the corresponding leachate-only systems yields an interesting observation. Exposure of *B. subtilis* to the pre-leached soluble Ag in fact resulted in much less growth inhibition when compared to those of the corresponding Ag NPs samples (Figure 1a). The presence of ~1.3 ppm Ag leachate for example, was benign to the cultures as they grew to a similar extent as the silver-free control cultures after 6 h. This was in contrast to the ~20% growth reduction of the bacteria when exposed to the corresponding 3 mg Ag L^{-1} NPs with comparable leached soluble Ag content. At higher exposure, the bacterial growth in 4 ppm Ag leachate system was ~85% relative to the control cultures (refer to Figure 1b for growth profile), in contrast to the near complete growth suppression observed in the corresponding 10 mg Ag L^{-1} NPs system. Even doubling the concentration of Ag leachate to 8.3 ppm only slightly reduced the bacterial growth to ~75%. The findings suggest predominant cytotoxicity contribution from the undissolved Ag particulates, rather than that arising from the leached soluble Ag. Further antimicrobial simulation with an equivalent concentration of soluble Ag from $AgNO_3$ salt as shown in Figure 1a, saw more severe growth inhibiting activity of the salt. In the presence of 4 ppm soluble Ag from $AgNO_3$ for example, ~25% *B. subtilis* growth was

observed relative to the control cultures after 6 h (growth profile is shown in Figure 1b), in contrast to the ~85% growth in the leachate system with comparable Ag concentration. Such differences in cytotoxicity may arise from unique cellular physiological responses to the different silver species; the leached soluble Ag and the undissolved Ag particulates from Ag NPs, and the soluble silver from silver salt, as investigated in the following.

Dynamic stimulation of cellular oxidative stress and cell death

We carried out dynamic tracking of intracellular reactive oxygen species (ROS) generation (measured by H_2DCFDA assay) and cell viability (measured by propidium iodide assay, whereby PI enters cells with damaged cytoplasmic membrane, which is indicative of cell death) over the 6 h growth course of *B. subtilis* in the presence of the various forms of silver; the Ag NPs (MIC_{95} 10 mg Ag L^{-1} as reference point, contained 4 ppm leached Ag), its corresponding Ag leachate system (4 ppm Ag) and the equivalent $AgNO_3$ system (4 ppm Ag).

The solid Ag particulates and the leached soluble Ag

At 5 min exposure to 10 mg Ag L^{-1}NPs, a 3-fold higher cellular ROS level was detected in *B. subtilis* relative to the basal ROS levels of the silver-free control cultures, which are by-products of aerobic metabolism in bacteria (Choi and Hu 2008, Gunawan et al. 2011, Eckhardt et al. 2013) (Figure 2a, 2b, 4a). Within 30 min of Ag NPs exposure, the cellular ROS level doubled to ~6-fold of the control. A secondary oxidative stress response, the cellular ROS stimulation has been increasingly realized as one of the major cellular toxicological responses to Ag NPs in bacteria (Choi and Hu 2008, Hwang et al. 2008, Lemire et al. 2013, Gunawan et al. 2013b). The ROS generation is thought to result from destruction of the iron-sulfur [4Fe-4S] clusters of proteins by Ag metal (Xu and Imlay 2012, Lemire et al. 2013) and in turn, releasing the Fenton-active free Fe into the cytoplasm for subsequent reaction with cellular H_2O_2 to produce hydroxyl

radicals ($OH^{\bullet}$) (Imlay et al. 1988). Alternatively, indirect destruction of the iron-sulfur clusters could result from inhibition of respiratory enzymes by Ag NPs in bacteria (Li et al. 2010, 2011). The resulting premature leakage of electrons to oxygen will generate superoxide radicals ($O_2^{\bullet-}$) (Imlay 2003) that in turn again, induces the release of free Fe from iron-sulfur clusters in proteins (Kohanski et al. 2007). Indeed, there have been reports on the cytoplasmic presence of the solid Ag particulates upon bacterial exposure to Ag NPs, as well as the presence of the solids within the bacterial membrane layers (Morones et al. 2005, Grigor'eva et al. 2013, Pal et al. 2007). Here, 75-90% PI-positive non-viable bacteria had been detected within 5 to 30 min exposure to Ag NPs, then close to 100% bactericidal or cell death toxicity at as early as 1 h exposure (Figure 2a, 2b, 4b), which indicates cytoplasmic membrane as one of the target destruction sites of the Ag NPs-stimulated cellular ROS (1-8% non-viable cells were detected in the control cultures over the 6 h growth course) (D'Autreaux et al. 2007, Lemire et al. 2013). As expected, the levels of cellular ROS drastically dropped following the rapid high level stimulation, with the majority if not all of the bacterial population were already killed (Sintubin et al. 2011, Gunawan et al. 2013b). Up to this stage, the data suggest that the generation of high levels of cellular ROS and associated bacteria killing was likely to be responsible for the near complete suppression of *B. subtilis* growth (Figure 1a, 1b).

Interestingly, such cellular ROS stimulation was absent in the bacteria when studied in the corresponding 4 ppm Ag leachate system. Over the 6 h growth course, only basal ROS levels, comparable to those of the silver-free control cultures were detected (Figure 2a, 3a, 4a) and not surprisingly, the little to no changes in the fraction of non-viable cells relative to the control (Figure 2a, 3a, 4b). The stimulation of lethal levels of cellular oxidative stress by the presence of solid Ag particulates therefore suggests their substantial contribution to the cytotoxicity effects observed in the growth studies. Recalling the observed ~15% growth inhibition of the bacteria in

the presence of 4 ppm Ag leachate (Figure 1a, 1b), it would be reasonable to deduce that the exposure only resulted in sub-lethal cytotoxicity, causing a minor fraction of the viable cells uncultivable or slowly proliferating, as further indicated by our growth prediction based on the fraction of viable cells (Figure S2). Indeed, doubling the Ag leachate concentration to 8.3 ppm still saw typical cellular ROS (Figure 3c, 4a inset) and dead cells (Figure 3c, 4b inset) detection as those of the control cultures, despite the slightly higher growth suppression, at ~25% (Figure 1a).

The leached soluble Ag and silver salt

The minimal cellular ROS stimulation was also seen upon exposure of *B. subtilis* to the equivalent 4 ppm soluble Ag from $AgNO_3$. Similar to the 4 ppm Ag leachate system, no elevated level of cellular ROS was observed over the 6 h growth course relative to the control cultures (Figure 2a, 3b, 4a). Unlike the leachate samples however, up to ~40% non-viable cells were detected in the salt system (Figure 3b, 4b), indicating attacks on cytoplasmic membrane (Eckhardt et al. 2013). Considering the comparable Ag content, such discrepancies in cytotoxicity are most likely to result from differences in the chemical speciation of the soluble silver, as herein described. Our Ag NPs leaching study (at the MIC_{95} 10 mg Ag L^{-1} NPs) in the individual culture medium components revealed a characteristic trend of complexation-assisted dissolution of nanoparticles (Gunawan et al. 2011), with higher extent of Ag leaching in the peptide-rich components, in particular tryptone (90% leaching relative to the total added Ag), compared to those in the deionized water (60% leaching) or NaCl (10% leaching) (Figure 4c). A soft Lewis acid, Ag(I) forms silver-peptide complexes upon its release from NPs (Bolea et al. 2014), which is most likely to result from its strong affinity to the NH_x donor groups of histidine (NH^+), arginine ($-NH_2^+$) and lysine ($-NH_3^+$) amino acids and also to the thiol ($-S^-$) donor groups of cysteine and methionine amino acids (Eckhardt et al. 2013). Silver-peptide complexes also form with $AgNO_3$ (Bolea et al. 2014), with a fraction of silver is thought to remain as free ions in

the organic-rich medium (Percival et al. 2005). Thermodynamically feasible, the co-existence of free metal ions and organo metal complexes has been reported for the chemical speciation of soluble copper salts, also a soft Lewis acid metal, in similar culture medium as that used here (Gunawan et al. 2011) (note that the current technology for elemental analysis does not differentiate free Ag ions to those locked in organo complexes (Eckhardt et al. 2013)). When compared to free Ag ions, the hindered transport of the bulkier silver-peptide complexes into bacteria (Solioz and Odermatt 1995) is thought to be at least in part, responsible for the passivated, in this case, sub-lethal cytotoxicity of the Ag leachate. Unlike free Ag ions, research indicates that soluble organo Ag complexes are not recognized by the P-type ATPase transporter present in bacteria (Luoma 2008). As also observed in the current study with the $AgNO_3$ systems, exposure of bacteria to Ag ions has been reported to suppress their proliferation, which was indicated to result from a ROS-independent inhibition of metabolic enzymes (dehydratases) (Xu and Imlay 2012), the lack of cellular ROS stimulation also apparent in this work. Further, complete suppression of *B. subtilis* growth was seen at 8.3 ppm Ag from $AgNO_3$ (Figure 1a), despite there being no change in the fraction of non-viable cells when compared to the 4 ppm Ag exposure (Figure 3d, 4b inset). Our growth prediction based on the fraction of viable cells indicates major presence of non- or slowly proliferating viable cells with the $AgNO_3$ exposure (Figure S2). This loss in replication could also result from the known interactions of Ag ions with DNA in bacteria (most likely with the phosphorus moieties) causing DNA condensation (Feng et al. 2000). The seemingly higher cytotoxic effects of Ag ions as compared to the organo Ag complexes are in agreement with other bacterial studies, whereby extracellular presence of thiol-containing reduced gluthathione (GSH) as silver complexing agent lowered the antimicrobial activity of Ag ions on the Gram-positive *Staphylococcus aureus* and the Gram-negative *Escherichia coli* and *Pseudomonas aeruginosa* (Mulley et al. 2014). Finally, the detection of only basal cellular ROS levels in the $AgNO_3$ exposure systems, even at the double 8.3 ppm Ag (Figure 3d, 4a inset), rules out the oxidative stress stimulation as the main

mechanisms of $AgNO_3$ cytotoxicity. Indeed, studies have found no differences in the antimicrobial activity of Ag ions under aerobic and anaerobic conditions on bacteria (Sintubin et al. 2011).

Conclusions

Here, we report multiple cytotoxicity origins of Ag NPs towards bacteria. Presence of undissolved Ag particulates in a biological environment is not inert. In their presence, rapid generation of lethal cellular ROS levels were detected in bacteria, while the corresponding leached soluble Ag, being locked in organo complexes, only imparts sub-lethal cytotoxicity. The observed differences in bacterial toxicological responses to the solid *versus* soluble Ag corroborate earlier reports on the distinct extent of growth inhibiting activity of the Ag NPs' soluble and solid components (Gunawan et al. 2009, Sotiriou and Pratsinis 2010). With regard to the widespread use of Ag NPs, the resolved unique toxicological responses are expected to result in better recognition of the antimicrobial potency of the nanoparticles in real-world settings and importantly, the long-term impact. Research inquiries have shown elevated and persistent presence of silver in wounds, bladder and even in sewage and estuaries, being associated with the intended or in some cases, accidental release from nanosilver applications; the use of wound dressings, pesticides and washing machines are among the examples (Chen et al. 2004, Trop et al. 2006, Reidy et al. 2013, Donner et al. 2015, Beddow et al. 2017). The current findings imply bacterial toxicological responses to not only the leached soluble Ag, but also the Ag particulates in the microbial habitats. Indeed, studies have observed disruptions in the dynamic and balance of microbial communities from natural aquatic waters upon exposure to nanosilver (Das et al. 2012, Beddow et al. 2017), with the work also detecting presence of soluble Ag and aggregates of Ag from nanosilver in these environmental samples (Beddow et al. 2017). The resolved toxicological responses is key to the elucidation of the recently discovered bacterial potential for adaptation to Ag NPs cytotoxicity (Das et al. 2012, Gunawan et al. 2013b). Finally, the work

highlights the unsuitability of soluble silver salt as model material for Ag NPs cytotoxicity in biological environments, noting a distinct ROS-independent antimicrobial characteristic of soluble Ag when supplied as $AgNO_3$ salt.

Acknowledgments

This work was produced with the financial assistance of the Australian Research Council under the ARC Australian Laureate Fellowship Program and the University of Technology Sydney under the Chancellor's Postdoctoral Research Fellowship Program.

Declaration of interest

The authors declare no conflict of interest.

References

Beddow J, Stolpe B, Cole PA, Lead JR, Sapp M, Lyons BP, et al. 2017. Nanosilver inhibits nitrification and reduces ammoniaoxidising bacterial but not archaeal *amoA* gene abundance in estuarine sediments. Environ Microbiol 19: 500-510.

Benn TM, Westerhoff P. 2008. Nanoparticle silver released into water from commercially available sock fabrics. Environ Sci Technol 42: 4133-4139.

Benn T, Cavanagh B, Hristovski K, Posner JD, Westerhoff P. 2010. The release of nanosilver from consumer products used in the home. J Environ Qual 39: 1875-1882.

Bolea E, Jiménez-Lamana J, Laborda F, Abad-Álvaro I, Bladé C, Arola L, et al. 2014. Detection and characterization of silver nanoparticles and dissolved species of silver in culture medium and cells by AsFIFFF-UV-Vis-ICPMS: application to nanotoxicity tests. Analyst 139: 914-922.

Bondarenko O, Ivask A, Käkinen A, Kurvet I, Kahru A. 2013. Particle-cell contact enhances antibacterial activity of silver nanoparticles. PLoS One 8: e64060.

Chen J, Han CM, Yu CH. 2004. Change in silver metabolism after the application of nanometer silver on burn wound. Chin J Burns 20: 161-163.

Choi O, Hu Z. 2008. Size dependent and reactive oxygen species related nanosilver toxicity to nitrifying bacteria. Environ Sci Technol 42: 4583-4588.

Das P, Williams CJ, Fulthorpe RR, Hoque ME, Metcalfe CD, Xenopoulos MA. 2012. Changes in bacterial community structure after exposure to silver nanoparticles in natural waters. Environ Sci Technol 46: 9120-9128.

D'Autreaux B, Toledano MB. 2007. ROS as signalling molecules: mechanisms that generate specificity in ROS homeostasis. Nat Rev Mol Cell Biol 8: 813-824.

Deardorff J, 2014. Some antibacterials come with worrisome silver lining. Chicago Tribune, 16 Feb. Available from: http://articles.chicagotribune.com/2014-02-16/health/ct-nanosilver-met-20140216_1_consumer-products-other-antibiotic-drugs-germs

Donner E, Scheckel K, Sekine R, Popelka-Filcoff RS, Bennett JW, Brunetti G, et al. 2015. Non-labile silver species in biosolids remain stable throughout 50 years of weathering and ageing. Environ Pollut 205: 78-86.

Eckhardt S, Brunetto PS, Gagnon J, Priebe M, Giese B, Fromm KM. 2013. Nanobio silver: its interactions with peptides and bacteria, and its uses in medicine. Chem Rev 113: 4708-4754.

Faunce T, Watal A. 2010. Nanosilver and global public health: international regulatory issues. Nanomedicine 5: 617-632.

Feng QL, Wu J, Chen GQ, Cui FZ, Kim TN, Kim JO. 2000. A mechanistic study of the antibacterial effect of silver ions on *Escherichia coli* and *Staphylococcus aureus*. J Biomed Mater Res 52: 662-668.

Ge L, Li Q, Wang M, Ouyang J, Li X, Xing MMQ. 2014. Nanosilver particles in medical applications: synthesis, performance, and Toxicity. Int J Nanomed 9: 2399-2407.

Grigor'eva A, Saranina I, Tikunova N, Safonov A, Timoshenko N, Rebrov A, et al. 2013. Fine mechanisms of the interaction of silver nanoparticles with the cells of *Salmonella typhimurium* and *Staphylococcus aureus*. Biometals 26: 479-488.

Gunawan C, Teoh WY, Marquis CP, Lifia J, Amal R. 2009. Reversible antimicrobial photoswitching in nanosilver. Small 5: 341-344.

Gunawan C, Teoh WY, Marquis CP, Amal R. 2011. Cytotoxicity origin of copper(II) oxide nanoparticles: comparative studies with micron-sized particles, leachate, and metal Salts. ACS Nano 5: 7214-7225.

Gunawan C, Teoh WY, Ricardo, Marquis CP, Amal R. 2013a. Zinc oxide nanoparticles induce cell filamentation in *Escherichia coli.* Part Part Syst Charact 30: 375-380.

Gunawan C, Teoh WY, Marquis CP, Amal R. 2013b. Induced adaptation of *Bacillus* sp. to antimicrobial nanosilver. Small 9: 3554-3560.

Gunawan C, Marquis CP, Amal R, Sotiriou GA, Rice SA, Harry EJ. 2017. Widespread and indiscriminate nanosilver use: genuine potential for microbial resistance. ACS Nano 11: 3438-3445.

Hajipour MJ, Fromm KM, Ashkarran AA, Jimenez de Aberasturi D, de Larramendi IR, Rojo T, et al. 2012. Antibacterial properties of nanoparticles. Trends Biotechnol 30: 499-511.

Hwang ET, Lee JH, Chae YJ, Kim YS, Kim BC, Sang BI, et al. 2008. Analysis of the toxic mode of action of silver nanoparticles using stress-specific bioluminescent bacteria. Small 4: 746-750.

Imlay J, Chin S, Linn S. 1988. Toxic DNA damage by hydrogen peroxide through the Fenton reaction *in vitro* and *in vivo*. Science 240: 640-642.

Imlay JA. 2003. Pathways of oxidative damage. Annu Rev Microbiol 57: 395-418.

Ivask A, Elbadawy A, Kaweeteerawat C, Boren D, Fischer H, Ji Z, et al. 2014. Toxicity mechanisms in *Escherichia coli* vary for silver nanoparticles and differ from ionic silver. ACS Nano 8: 374-386.

Kohanski MA, Dwyer DJ, Hayete B, Lawrence CA, Collins JJ. 2007. A common mechanism of cellular death induced by bactericidal antibiotics. Cell 130: 797-810.

Lemire JA, Harrison JJ, Turner RJ. 2013. Antimicrobial activity of metals: mechanisms, molecular targets and applications. Nat Rev Microbiol 11: 371-384.

Levard C, Mitra S, Yang T, Jew AD, Badireddy AR, Lowry GV, et al. 2013. Effect of chloride on the dissolution rate of silver nanoparticles and toxicity to *E. coli*. Environ Sci Technol 47: 5738-5745.

Li WR, Xie XB, Shi QS, Zeng HY, Ou-Yang YS, Chen YB. 2010. Antibacterial activity and mechanism of silver nanoparticles on *Escherichia coli*. Appl Microbiol Biotechnol 85: 1115-1122.

Li WR, Xie XB, Shi QS, Duan SS, Ou-Yang YS, Chen YB. 2011. Antibacterial effect of silver nanoparticles on *Staphylococcus aureus*. Biometals 24: 135-141.

Liu J, Wang Z, Liu FD, Kane AB, Hurt RH. 2012. Chemical transformations of nanosilver in biological environments. ACS Nano 6: 9887-9899.

Luoma SN, 2008. Silver nanotechnologies and the environment: old problems or new challenges? The PEW Charitable Trusts. Available from: https://www.nanotechproject.org/process/assets/files/7036/nano_pen_15_final.pdf [Accessed 11 December 2016]

Mirzajani F, Ghassempour A, Aliahmadi A, Esmaeili MA. 2011. Antibacterial effect of silver nanoparticles on *Staphylococcus aureus*. Res Microbiol 162: 542-549.

Morones JR, Elechiguerra JL, Camacho A, Holt K, Kouri JB, Ramírez JT, et al. 2005. The bactericidal effect of silver nanoparticles. Nanotechnology 16: 2346-2353.

Mulley G, Jenkins ATA, Waterfield NR. 2014. Inactivation of the antibacterial and cytotoxic properties of silver ions by biologically relevant compounds. PLoS One 9: e94409.

Pal S, Tak YK, Song JM. 2007. Does the antibacterial activity of silver nanoparticles depend on the shape of the nanoparticle? A study of the Gram-negative bacterium *Escherichia coli*. Appl Environ Microbiol 73: 1712-1720.

Percival SL, Bowler PG, Russell D. 2005. Bacterial resistance to silver in wound care. J Hosp Infect 60: 1-7.

Quadros ME, Pierson R, Tulve NS, Willis R, Rogers K, Thomas TA, et al. 2013. Release of silver from nanotechnology-based consumer products for children. Environ Sci Technol 47: 8894-8901.

Reidy B, Haase A, Luch A, Dawson KA, Lynch I. 2013. Mechanisms of silver nanoparticle release, transformation and toxicity: a critical review of current knowledge and recommendations for future studies and applications. Materials 6: 2295-2350.

Silver S. 2003. Bacterial silver resistance: molecular biology and uses and misuses of silver compounds. FEMS Microbiol Rev 27: 341-353.

Sintubin L, De Gusseme B, Van der Meeren P, Pycke BFG, Verstraete W, Boon N. 2011. The antibacterial activity of biogenic silver and its mode of action. Appl Microbiol Biotechnol 91: 153-162.

Solioz M, Odermatt A. 1995. Copper and silver transport by CopB-ATPase in membrane vesicles of *Enterococcus hirae*. J Biol Chem 270: 9217-9221.

Sondi I, Salopek-Sondi B. 2004. Silver nanoparticles as antimicrobial agent: a case study on *E. coli* as a model for Gram-negative bacteria. J Colloid Interface Sci 275: 177-182.

Sotiriou GA, Pratsinis SE. 2010.Antibacterial activity of nanosilver ions and particles. Environ Sci Technol 44: 5649-5654.

Sotiriou GA, Meyer A, Knijnenburg JTN, Panke S, Pratsinis SE. 2012. Quantifying the origin of released Ag+ ions from nanosilver. Langmuir 28: 15929−15936.

Trop M, Novak M, Rodl S, Hellbom B, Kroell W, Goessler W. 2006. Silver-coated dressing Acticoat caused raised liver enzymes and argyria-like symptoms in burn patient. J Trauma-Injury Infect Crit Care 60: 648-652.

Xiu ZM, Zhang QB, Puppala HL, Colvin VL, Alvarez PJJ. 2012. Negligible particle-specific antibacterial activity of silver nanoparticles. Nano Lett 12: 4271-4275.

Xu FF, Imlay JA. 2012. Silver(I), mercury(II), cadmium(II), and zinc(II) target exposed enzymic iron-sulfur clusters when they toxify *Escherichia coli*. Appl Environ Microbiol 78: 3614-3621.

Consumer Products Inventory – Project on Emerging Nanotechnologies. Available from: http://www.nanotechproject.org/cpi [accessed 1 March 2017].

Supplementary material is available: Supplementary Figure S1, S2 and S3.

Figure captions

Figure 1. Bacterial growth in the presence of Ag NPs, Ag NPs leachate, silver salt and leaching of Ag NPs. **(a)** Growth of *B. subtilis* (6 h) relative to cell-only control upon exposure to Ag NPs (3, 6, 8, 10 mg Ag L^{-1}), Ag leachate from NPs and $AgNO_3$ as a function of soluble silver detected in the bacterial exposure systems (the growth studies were performed in LB medium). **(b)** Growth profiles of the bacteria in the presence of 10 mg Ag L^{-1} NPs (4 ppm Ag leached into medium at equilibrium), 4 ppm Ag leachate from NPs and 4 ppm Ag from $AgNO_3$. Also shown is the cell-only control growth profile (dashed line). The growth in the presence of Ag was normalised to the extent of growth of the control (in colony forming units, cfu). **(c)** The corresponding equilibrium leaching of Ag NPs in the bacterial exposure systems, shown in the inset is the leaching profile for 10 mg Ag L^{-1} NPs. Each data point in (a), (b), (c) is the average of triplicate experiments with error bars representing the maximum and minimum values detected. The growth studies were performed under dark conditions to render the TiO_2 support

photocatalytically inactive and the benign effect of the TiO_2 support on *B. subtilis* growth had been confirmed (Gunawan et al. 2013b). The growth studies were reproduced on different days with unique bacterial inoculum and particle preparations.

Figure 2. Detection of cellular reactive oxygen species (ROS, H_2DCFDA staining, green cells) and cell death (PI staining, red cells) of *B. subtilis* over its growth course: **(a)** cell-only control and **(b)** in the presence of 10 mg Ag L^{-1} NPs. All stained samples were imaged at comparable cell concentrations (scale bars = 50 µm).

Figure 3. Detection of cellular reactive oxygen species (ROS, H_2DCFDA staining, green cells) and cell death (PI staining, red cells) of *B. subtilis* over its growth course, in the presence of: **(a)** 4 ppm Ag leachate from NPs (equivalent leachate to 10 mg Ag L^{-1} NPs exposure), **(b)** 4 ppm Ag from $AgNO_3$, **(c)** 8.3 ppm Ag leachate from NPs and **(d)** 8.3 ppm Ag from $AgNO_3$. All stained samples were imaged at comparable cell concentrations (scale bars = 50 µm).

Figure 4. **(a)** Dynamic stimulation of cellular ROS in *B. subtilis* measured by H_2DCFDA assay over its growth course (5, 30 min and 1, 3, 4.5, 6 h) upon exposure to 10 mg Ag L^{-1} NPs (4 ppm Ag leached into medium at equilibrium), 4 ppm Ag leachate from NPs and 4 ppm Ag from $AgNO_3$. The detected cellular ROS was normalised to the basal ROS levels of the cell-only control growth. Shown in the inset is cellular ROS detected in the presence of 8.3 ppm Ag leachate from NPs and 8.3 ppm Ag from $AgNO_3$. **(b)** The corresponding dynamic cell death detection probed by PI staining of *B. subtilis* throughout its growth course. Also shown is the fraction of dead cells detected for the cell-only control. Statistical analysis of the data was performed with one-way ANOVA followed by Dunnett's posthoc analysis in Prism (GraphPad) (Figure S3). The experiments in (a) and (b) were reproduced on different days with unique bacterial inoculum and particle preparations. **(c)** Leaching profile of 10 mg Ag L^{-1} NPs in cell-

free individual components of the Luria Bertani (LB) culture medium (5 g L^{-1} NaCl, 5 g L^{-1} yeast extract, 10 g L^{-1} tryptone dissolved in deionized water). Each data point in (a), (b), (c) is the average of triplicate batches with the error bars representing the maximum and minimum.